Selective potentiation of the $(\alpha4)_3(\beta2)_2$ nicotinic acetylcholine receptor response by NS9283 analogues

Rebecca Appiani [†], *Franco Viscarra* [#,§], *Philip C. Biggin* [§], *Isabel Bermudez* [#], *Alessandro Giraudo* [†], *Marco Pallavicini* [†], *and Cristiano Bolchi* [†*]

*Corresponding author: cristiano.bolchi@unimi.it

[†] Dipartimento di Scienze Farmaceutiche, Università degli Studi di Milano, via Mangiagalli 25, I-20133 Milano, Italy

[#] Department of Biological and Medical Sciences, Oxford Brookes University, Oxford OX3 0BP, U.K.

[§] Structural Bioinformatics and Computational Biochemistry Unit, Department of Biochemistry, University of Oxford, Oxford OX1 3QU, U.K.

KEYWORDS: 1,2,4-oxadiazoles, nicotinic acetylcholine receptor, unorthodox site, α4/α4 site, voltage-clamp, molecular dynamics, NS9283.

Abstract

NS9283, 3-(3-pyridyl)-5-(3-cyanophenyl)-1,2,4-oxadiazole, is a selective positive allosteric modulator of $(\alpha4)_3(\beta2)_2$ nicotinic acetylcholine receptors (nAChR). It has good subtype selective therapeutic potential afforded by its specific binding to the unique α4-α4 subunit interface present in

the $(\alpha4)_3(\beta2)_2$ nAChR. However, there is currently a lack of structure activity relationships (SAR) studies aimed at developing a class of congeners endowed with the same profile of activity that can help consolidate the druggability of the α4-α4 subunit interface. In this study, new NS9283 analogues were designed, synthesized, and characterized for their ability to selectively potentiate the ACh activity at heterologous $(\alpha4)_3(\beta2)_2$ nAChRs *vs* nAChR subtypes $(\alpha4)_2(\beta2)_3$, α5α4β2 and α7. With few exceptions, all the NS9283 analogues exerted positive modulation of the $(\alpha4)_3(\beta2)_2$ nAChR ACh-evoked responses. Above all, those modified at the 3-cyanophenyl moiety by replacement with 3-nitrophenyl (**4**), 4-cyanophenyl (**10**), and *N*-formyl-4-piperidinyl (**20**) showed the same efficacy as NS9283, although with lower potency. Molecular dynamic simulations of NS9283 and some selected analogues highlighted consistency between potentiation activity and pose of the ligand inside the α4-α4 site with the main interaction being with the complementary (-) side and induction of a significant conformational change of the Trp156 residue in the principal (+) side.

INTRODUCTION

The α4β2 nicotinic acetylcholine receptor (nAChR) is the most abundant subtype in the brain. Its implication in drug and nicotine addiction and in a range of severe central nervous system (CNS) disorders is widely documented, and partial α4β2 agonists are currently used as smoking deterrents and investigated for their therapeutic potential in the treatment of depressive symptoms, pain modulation and reduction of ethanol consumption. [1,2]

Relying on previously identified and characterized hits, and on available 3D structures of nAChR subtypes, our work has focused on developing partial agonists selective for α4β2 nAChR.[3-6] Partial agonists of α4β2 nAChR are more suitable for clinical application than full or super-agonists due to their wider therapeutic range and attenuated side effects. [4-6] More recently, we have developed α4β2 agonists with receptor-stoichiometry-selectivity. [7] The α4 and β2 subunits assemble into two forms, the $(\alpha4)_2(\beta2)_3$ stoichiometry, which has high sensitivity to activation by agonists (HS α4β2 nAChR),

and the $(\alpha4)_3(\beta2)_2$ stoichiometry, which has lower agonist sensitivity (LS α4β2 nAChR).[8-10] The differences in type and relative disposition of subunit interfaces between the two isoforms result in two stoichiometry-specific subunit interfaces (α4/α4 in LS α4β2; β2/β2 in HS α4β2, [11], which can be exploited to achieve isoform selective α4β2 nAChR effects. In principle, allosteric modulators binding at receptor-unique sites should be useful to discriminate the different effects mediated by the two isoforms, reducing doses and undesired effects of co-administered orthosteric agonists or simply sustaining the level of cholinergic tone without exogenous agonists, thus improving the druggability of the α4β2 nAChR.[12]

In this sense, the pyridinyl cyanophenyl oxadiazole NS9283 has been, and still is, one of the most studied compounds for the mechanism of selective LS α4β2 isoform potentiation and potential therapeutic applications. First reported as a positive allosteric modulator of the α4β2 nAChR in 2009,[13] it was better characterized three years later by the same researchers, who revealed, through its use, a differential distribution of the two α4β2 isoforms in the brain. [14] In addition, NS9283 showed a concentration-dependent increase of ACh evoked current peaks in the LS α4β2 receptors, with no positive modulatory effect on the HS isoform and no detectable signal when applied alone.[15] It emerged that NS9283 increases the potency but not the efficacy of ACh and reduces the recovery rate from ACh-induced desensitization.[16] Subsequently, a series of structural and functional studies established NS9283 as a stoichiometry selective positive modulator targeting the α4-α4 interface, a subunit interface capable of binding ACh and contributing to the activation of LS α4β2 receptors.[12,17,18] Additionally, NS9283 *in vivo* pharmacological characterization demonstrates reduction of nicotine self-administration, full nicotine substitution if co-administered with very low doses of orthosteric agonists, enhancement of the analgesic efficacy of nAChR agonists and cognitive improvement without exogenous agonist supplementation.[19,20] More recent mutational studies of LS α4β2 nAChR assembled from separate α4 and β2 subunits or fully concatenated α4 and β2 subunits suggest that the β2(+)-α4(-) subunit interface in LS α4β2 nAChR may act a transduction element for

potentiation, if not as a binding site for NS9283.[21]. However, the organisation of conserved aromatic residues in the β2+/α4- interface in HS α42 nAChR,[22] together with uncertainty on the location of agonist sites in concatenated receptors α4β2 nAChRs, [23] do not support the possibility of NS9283 binding to the β2+/α4- interface. [21] Thus, LS α4β2 sensitivity to potentiation by NS9283 is considered strictly dependent on the presence of α4-α4 sites. More recently, reports on NS9283 address its therapeutic potential to treat alcohol use disorder [24] and to strengthen, alone or with muscarinic agonists, cholinergic neurotransmission in CNS areas where it is vital for attention and cognitive functions.[25,26]

However, despite the great interest in NS9283 as a valuable pharmacological tool and drug discovery lead, to our knowledge, only one NS9283 structure activity relationships (SAR) investigation has been reported, [27] and this focused on the development of positive modulators for α4β2α5 nAChR, a receptor subtype that plays an important role in cognitive functions and control of nicotine intake.[25,28] Starting from this SAR study, based on single point changes made, one at a time, at the three cycles of NS9283, we have designed a series of new NS9283 analogues modified at the 3-cianophenyl residue (compounds **8**-**22**) or at the 3-pyridyl moiety (compounds **23**-**26**) and we have tested them and a selection of those previously reported (compounds **1**-**7**) for the ability to potentiate ACh response of LS α4β2 nAChRs. Here, we report their synthesis, pharmacological characterization and SAR analysis results, supported by computational studies revealing the key interactions of some of them at the α4-α4 intersubunit site.

Chart 1. NS9283 and its analogues modified at the peripheral rings

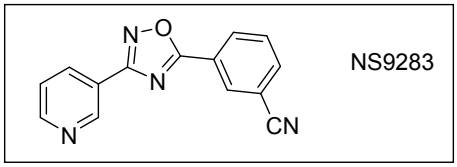

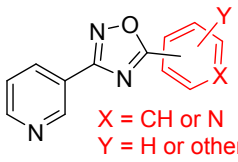

1	phenyl
2	3-pyridyl
3	2-NO_2-phenyl
4	3-NO_2-phenyl
5	4-NO_2-phenyl
6	3-F-phenyl
7	3,4-diF-phenyl
8	2-pyridyl
9	4-pyridyl
10	4-CN-phenyl
11	4-F-phenyl
12	3,4,5-triF-phenyl
13	2,3,4,5-tetraF-phenyl
14	3-NO_2-4-F-phenyl
15	3-F-4-NO_2-phenyl
16	6-F-3-pyridyl
17	3-carboxy-phenyl

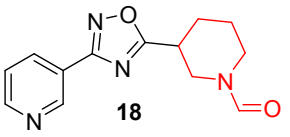
18

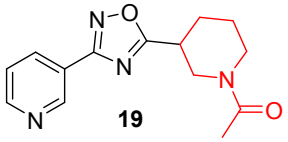
19

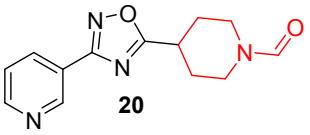
20

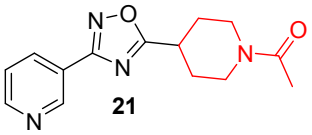
21

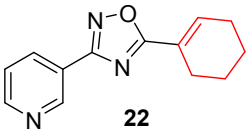
22

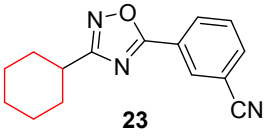
23

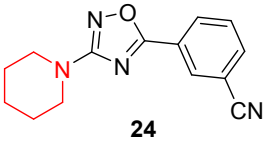
24

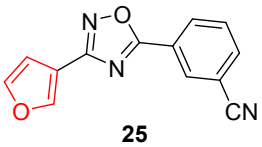
25

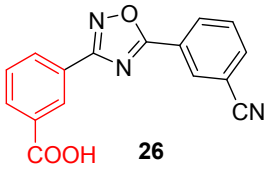
26

RESULTS AND DISCUSSION

Rational design

The binding mode and modulatory mechanism of NS9283 have been deeply investigated by combining x-ray crystallography, quantum mechanical calculations, mutational data, homology modeling and functional studies [17] and by docking analysis.[18] Overall, these studies indicate the key role of the hydrogen bond interactions established by the pyridine nitrogen of NS9283 with the α4 principal side and by its nitrile group, in particular, with the complementary α4 side. According to a homology model based on the crystal structure of the ACh-binding protein (AChBP) from *Lymnaea stagnalis* with NS9283, a favorable interaction of the CN group with H142, placed at the α4 minus side instead of a bulky valine residue in the corresponding β2-subunit position, underlies the α4-α4 *versus* α4-β2 interface selectivity of NS9283.[17] These results were confirmed by docking NS9283 at the α4-α4 interface of a successive LS nAChR homology model constructed from the structure of

the *L. stagnalis* AChBP crystallized with carbamylcholine, where NS9283 is positioned near H116 (H142 [17]).[18] Based on these indications, we opted for one-time modifications of the phenyl moiety and, secondly, of the pyridyl residue of NS9283 involving the presence and the position of electron withdrawing and hydrogen bond accepting substituents to further explore NS9283 SARs and discover new α4β2 LS isoform positive modulators. We started verifying the ability to enhance the response induced by ACh at this isoform by seven previously reported NS9283 analogues connoted by replacement of 3-cyanophenyl with 3-pyridyl, nitrophenyl and fluorophenyl residues and, for comparison, unsubstituted phenyl (compounds **1**-**7**).[27] Then, we widened the SAR analysis considering the same substituents but with different patterns of substitution (compounds **8**-**16**). Continuing with this NS9283 centric strategy, we decided to expand our investigation applying a virtual screening approach, namely a fragment-based drug discovery method, using BROOD 3.1.2.2. software and ChEMBL20 database, which is a manually curated chemical database of bioactive molecules with drug-like properties. The three fragments of NS9283, namely pyridine, oxadiazole and benzonitrile, were separated and the software substituted them with fragments maintaining productive binding, similar shape and attachment vectors, but exhibiting a range of other physicochemical properties. After running BROOD screening, the results were visualized using VIDA 4.4.0.4 software, which divided the potential hit compounds into clusters. From the clusters, we selected the compounds **17**-**22** and **23**-**26** as representative of cyanophenyl and pyridyl modifications, respectively. Particularly intriguing was the suggested non-obvious replacement of the cyanophenyl residue with an alicyclic N-acylated amine, such as N-formyl and N-acetylpiperidine, for the significant difference in interaction properties between the aromatic and aliphatic cycles and the resultant lower lipophilicity of the molecules though maintaining the presence of a hydrogen bond accepting (HBA) ring substituent.

Chemistry

The synthetic route to compounds **1**-**16** and **22** is shown in Scheme 1. Treatment of nicotinonitrile with hydroxylamine hydrochloride afforded pyridine-3-amidoxime (**27**), which was coupled with the

different acyl chlorides (**28-44**), previously obtained from the respective acids by reaction with thionyl chloride, to give compounds **1-16** and **22**. For the synthesis of compounds **18-21**, nipecotic acid and isonipecotic acid were treated with acetic anhydride to obtain the N-acetyl derivatives **46** and **48** or with acetic anhydride and formic acid to obtain the N-formyl derivatives **45** and **47**. The intermediates **45-48** were then converted in acyl chlorides (**49-52**) and reacted with **27** (Scheme 2). Compounds **23-26** were synthesized by the same route condensing 3-cyanobenzoyl chloride with the amidoxime obtained by reaction of hydroxylamine hydrochloride with, respectively, cyclohexyl cyanide (**53**), 1-piperidinecarbonitrile (**54**),3-furancarbonitrile (**55**) and 3-cyanobenzoic acid (**56**) (Scheme 3). Compound **17** was prepared by cyclization of **27** to 3-(3-pyridin3-yl)-1,2,4-oxadiazole (**57**), coupling with methyl 3-iodobenzoate (**58**) and ester saponification (Scheme 4).

Scheme 1. Synthetic route to 1-16 and 22

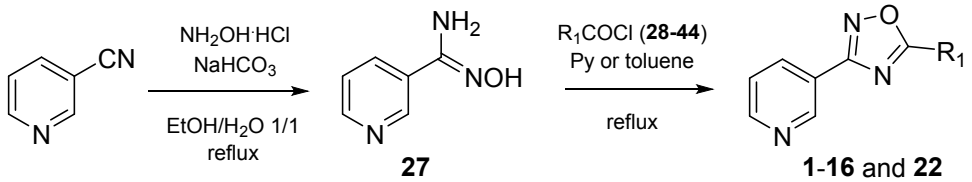

28	R_1 = phenyl	**32**	R_1 = 4-NO_2-phenyl	**36**	R_1 = 3,4-diF-phenyl	**40**	R_1 = 2,3,45-tetraF-phenyl
29	3-pyridyl	**33**	3-F-phenyl	**37**	4-CN-phenyl	**41**	3-NO_2-4-F-phenyl
30	2-NO_2-phenyl	**34**	3,4-diF-phenyl	**38**	4-F-phenyl	**42**	3-F-4-NO_2-phenyl
31	3-NO_2-phenyl	**35**	2-pyridyl	**39**	3,4,5-triF-phenyl	**43**	6-F-3-pyridyl
						44	1-cyclohexenyl

Scheme 2. Synthetic routes to 18-21

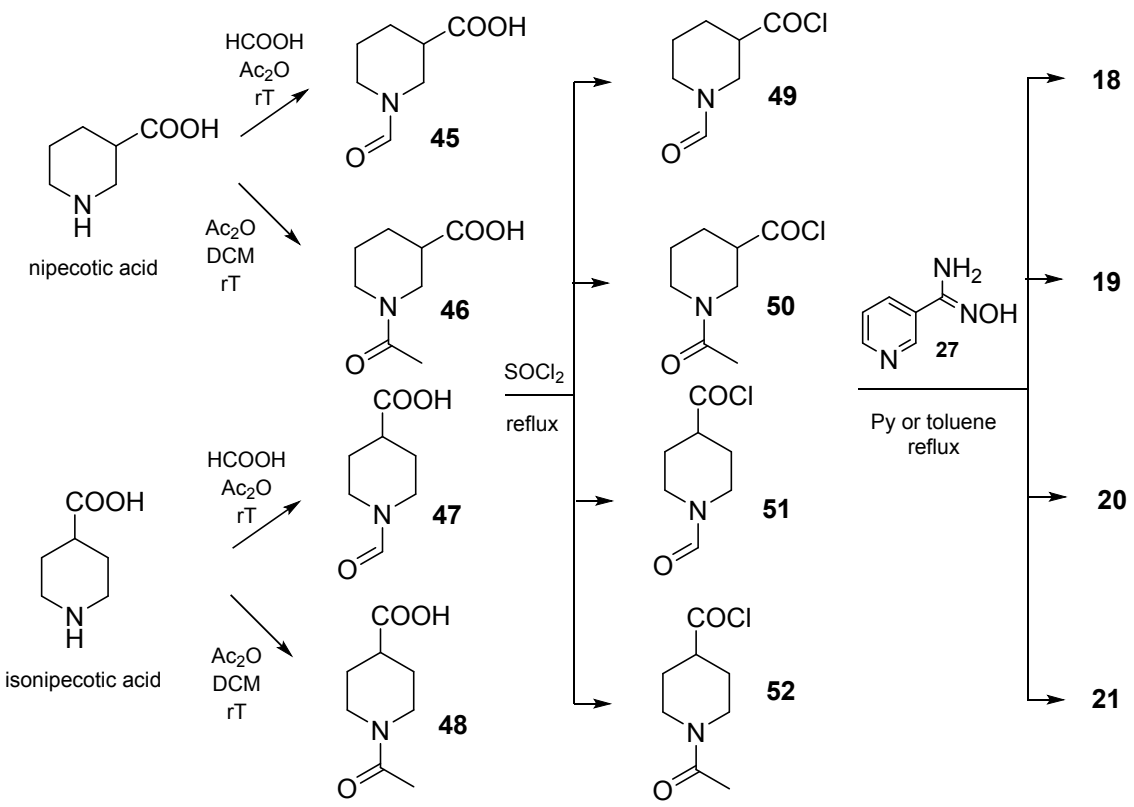

Scheme 3. Synthetic routes to 23-26

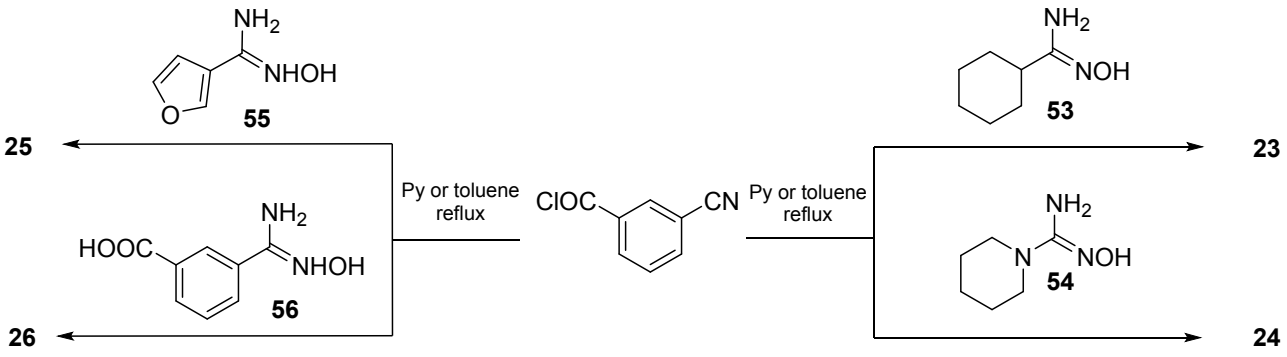

Scheme 4. Synthetic route to 17

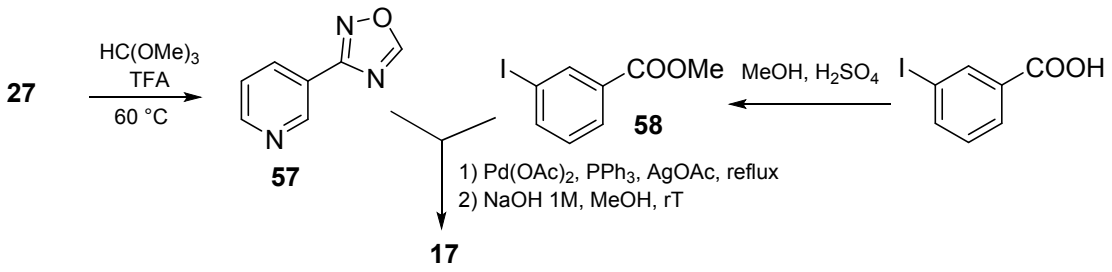

Functional assays

In the first set of experiments, NS9283 and its analogues shown in Chart 1 were evaluated for their ability to potentiate the current responses elicited by ACh 20% effective concentration (EC_{20}) at LS α4β2, HS α4β2, α5α4β2 or α7 nAChR expressed heterologously in *Xenopus laevis* oocytes. In these experiments, a single concentration was tested, 30 μM, a concentration at which NS9283 exerts maximal potentiation of EC_{20} ACh responses. NS9283 was assayed in parallel as an efficacious and selective positive allosteric modulator (PAM) of $(\alpha4)_3(\beta2)_2$ nAChR. Neither NS9283 or its analogues potentiated the EC_{20} ACh responses of HS α4β2, α5α4β2 or α7 nAChR (Figure 1). These results confirmed both the requirement of the α4-α4 interface for allosteric modulation of nAChR by the ligands, and the validity of this interface to develop uniquely selective LS α2β2 nAChR ligands. In addition, none of the ligands alone activated the receptors.

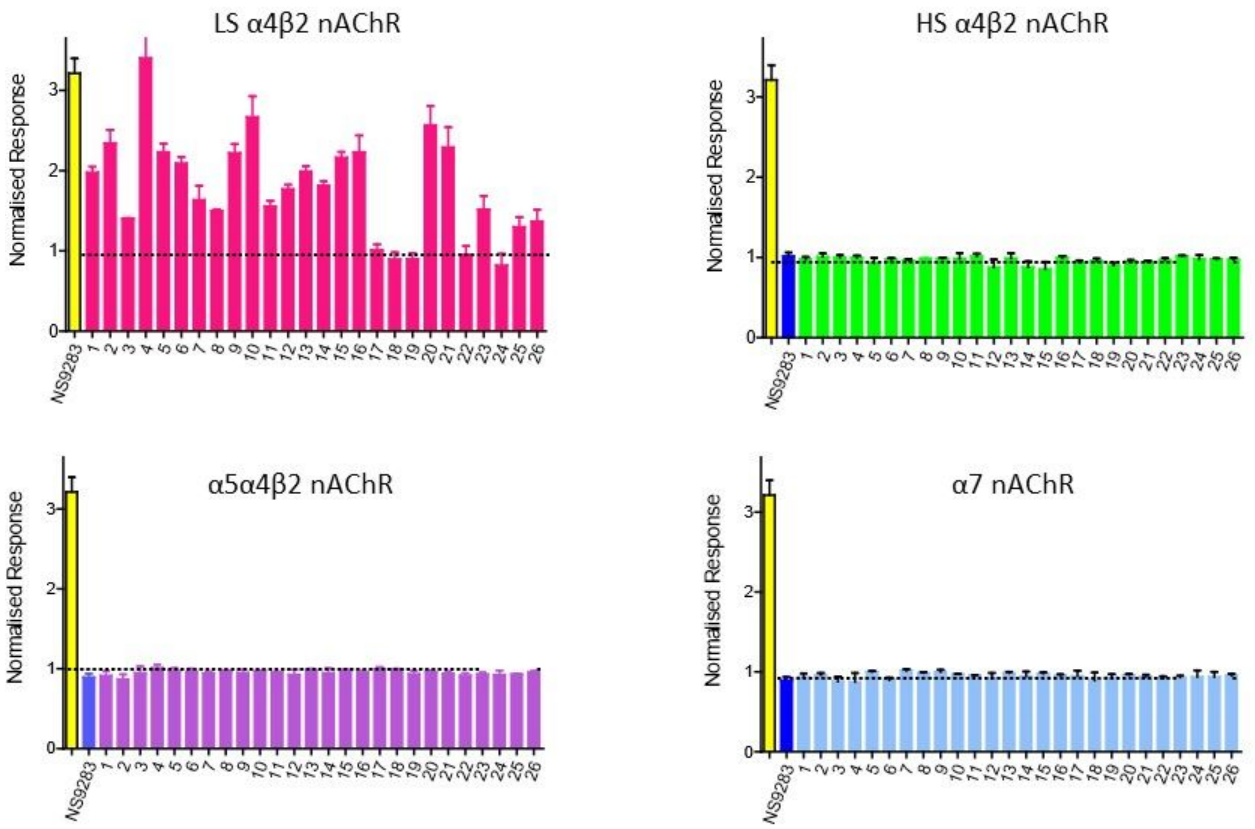

Figure 1. Activity of NS9283 and analogues at α4β2, α5α4β2 and α7 nAChRs. Ligands were tested for their effects on the ACh EC_{20} responses of LS $\alpha4\beta_2$, HS $\alpha4\beta_2$, α5α4β2 or α7 nAChR expressed heterologously in *Xenopus* oocytes using two-electrode voltage clamp recording procedures. For comparison purposes, the effects of NS9283 (yellow column) at LS α4β2 nAChR is included on the histograms for LS α4β2, HS α4β2, α5α4β2 and α7 nAChRs. All ligands were tested at 30 μM.

In contrast, ten analogues, all modified at the cyanophenyl portion of NS9283, potentiated the ACh EC_{20} responses of LS α4β2 nAChR with a relative efficacy comparable to that of NS9283 (Figure 1). Five of these resulted from substitution of 3-cyanophenyl with other substituted phenyl residues: 3- or 4-nitrophenyl (**4** and **5**), 3-fluorophenyl (**6**), 4-cyanophenyl (**10**), and 3-fluoro-4-nitrophenyl (**15**); three from replacement with pyridyl residues: 3- or 4-pyridyl (**2** and **9**), and 6-fluoro-3-pyridyl (**16**); two from fragment substitutions indicated by the fragment-based drug discovery (FBDD) approach with: N-formyl-4-piperidinyl (**20**) and N-acetyl-4-piperidinyl (**21**). The concentration effects of NS9283, seven analogues selected from the above ten (**2**, **4**, **5**, **9**, **10**, **20**, and **21**) and **19** were determined on LS α4β2 nAChR. Their 50% effective concentration (EC_{50}) and relative efficacy of potentiation are reported in Table 1. Figure 2A shows the concentration-response curves for the

analogues tested. For comparison purposes, Table 1 and Figure 2 show the concentration effects of NS9283 and an analogue that displayed no potentiating activity at LS α4β2 nAChR (analogue **19**). Typical traces responses for NS283, **4**, **19**, and **21** are shown in Figure 2B.

Table 1. Concentration effects of NS9283 and analogues on LS α4β2 nAChR. The concentration effects of the test compounds were determined on ACh responses elicited by an EC_{20} ACh concentration (30 μM). The data points were used to generate concentration-response plots from which EC_{50}, and relative efficacy of potentiation were estimated, as described in Methods. The relative efficacy of potentiation of the ligands was calculated as $(I_{ACh\ EC20}$ + ligand) $/I_{ACh\ EC20}$. Data for NS9283 and an inactive analogue (**19**) are included for comparison purposes. Values represent the mean ± SEM of 5-8 number of experiments carried out on oocytes from at least three different donors. Statistical analyses were carried out using one-way ANOVA with CHECKBonbeforri's or Dunnett's correction, as described in Methods. Statistical differences between the amplitude of the currents generated by ACh EC20 in the absence or presence of ligands is indicated by +. Asterisks indicate that the change in EC_{50} and/or relative efficacy between NS9283 and the analogues is statistically significant (*, $p < 0.05$).

Ligand	Potency (EC_{50}) μM 95% CI of Mean	Relative Efficacy of Potentiation 95% CI of Mean	Relative efficacy of analogues/Relative efficacy of NS9283
NS9283	3.43 (2.3-4.6)	3.21+ (2.8-3.6)	
2	6.17 (4.1-8.4)	2.25+,* (1.9-2.6)	0.44
4	7.67 (5.8-9.5)	3.40+,* (2.7-4.1)	1.05
5	6.27 (4.1-8.4)	2.13+ (1.8-2.5)	0.67
9	14.48 (6 -35)	2.27+,* (1.8-2.7)	0.71
10	19.20* (9-28)	3.07+ (0.27-5.74)	0.96
19	NA	1.02 (0.97-1.07)	0.32
20	34* (12-56)	3.3+ (1.48-5.11)	1.03
21	55* (11-98)	2.58+ (1.62-3.53)	0.8

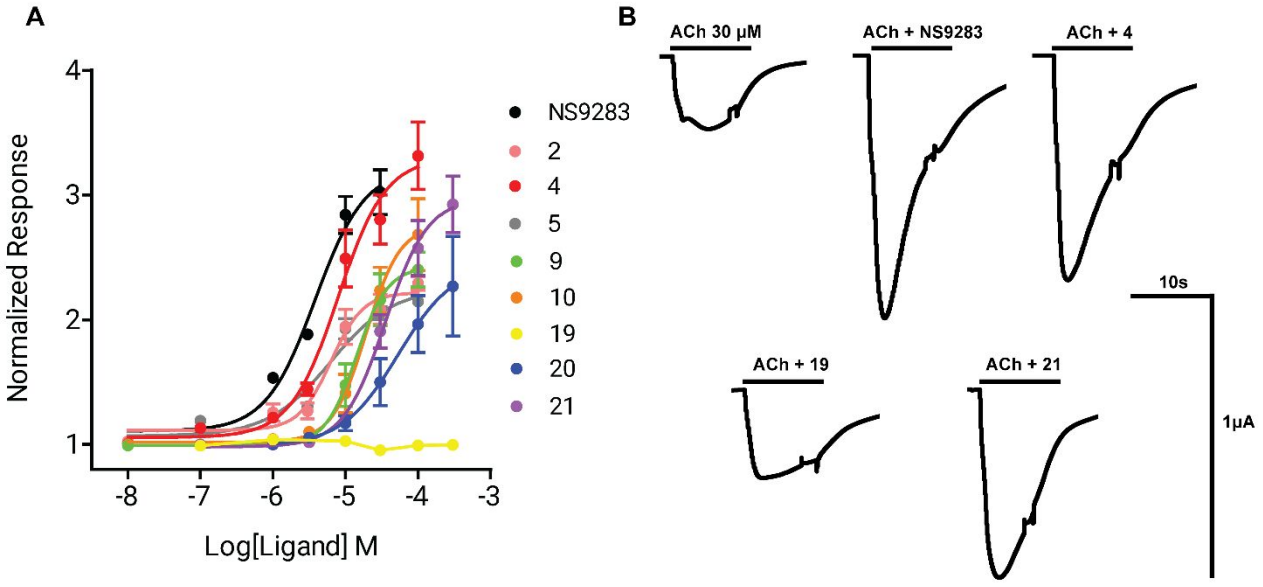

Figure 2. Effects of NS9283 and analogues on LS α4β2 nAChR. A) Concentration-dependent effects of ligands shown in Table 1 (NS9283, **2, 4**, **5**, **9**, **10**, **19**, **20** and **21**) on the responses of LS α4β2 nAChR to ACh EC_{20} (30 µM). B) Representative traces of 30 µM ACh-evoked current and 30 µM ACh-evoked currents in the presence of NS9283 or ligands **4**, **21** and **19**.

Overall, these data are consistent with the critical involvement of a hydrogen bond accepting function correctly positioned at the aromatic ring, as previously suggested for the interaction of 3-cyanophenyl residue with H116 of the complementary α4 side in the homology model of NS9283 binding.[18] Revealingly, shift of the substituents CN, NO_2, F and, to a minor extent, of the pyridyl nitrogen from the 3 to 4 position results in a decrease of ACh potentiation (cf. NS9283 with **10**, **4** with **5**, **6** with **11**, **2** with **9**) (Figure 1), thus suggesting a similar binding pattern for these compounds driven by the productive interaction of the hydrogen bond accepting atoms in the cycle bound to oxadiazole C(5). Conversely, when replacing 3-cyanophenyl with piperidinyl (compounds **18-21**), the HBA substituent, formyl or acetyl, has to be shifted from the 3 to 4 position: **20** and **21** show ACh potentiation, **18** and **19** are inactive (Figure 1).

Computational studies of NS9283 and ligands 4, 19, and 21

In an attempt to understand how the pattern of substitutions applied to the phenyl and pyperidine rings of NS9283 affects the interactions of these compounds with the α4-α4 interface, we performed computational studies focusing on NS9283, its two active analogues, 3-nitrophenyl (**4**) and N-acetyl-4-piperidinyl (**21**), and N-acetyl-3-piperidinyl (**19**), which is an inactive analogue of **21**.

The cluster densities resulting from the replica exchange simulations (see Methods) show one major cluster for NS9283, ligand **4**, and ligand **19**, and two similarly populated clusters for ligand **21** (Supplementary Table S1). The conformation predicted for NS9283 (Figure 3A) shows the ligand mainly interacting with the complementary (-) side of the binding site and remains highly stable in the subsequent unbiased simulation (Supplementary Figure S1A). Furthermore, the conformation is consistent across the different repeats (Supplementary Figure S2). The strongest interactions are with the residues W62, R86, H116, Q124, and T126 (Supplementary Figure S3A and S3B), which have been previously identified as important residues for the potentiating effect of NS9283.[17] Even though the ligand pose differs significantly from the one previously reported in the literature, it is worth noting that the current work was done using the α4β2 nAChR structure, which was not available at the time of the previous study.

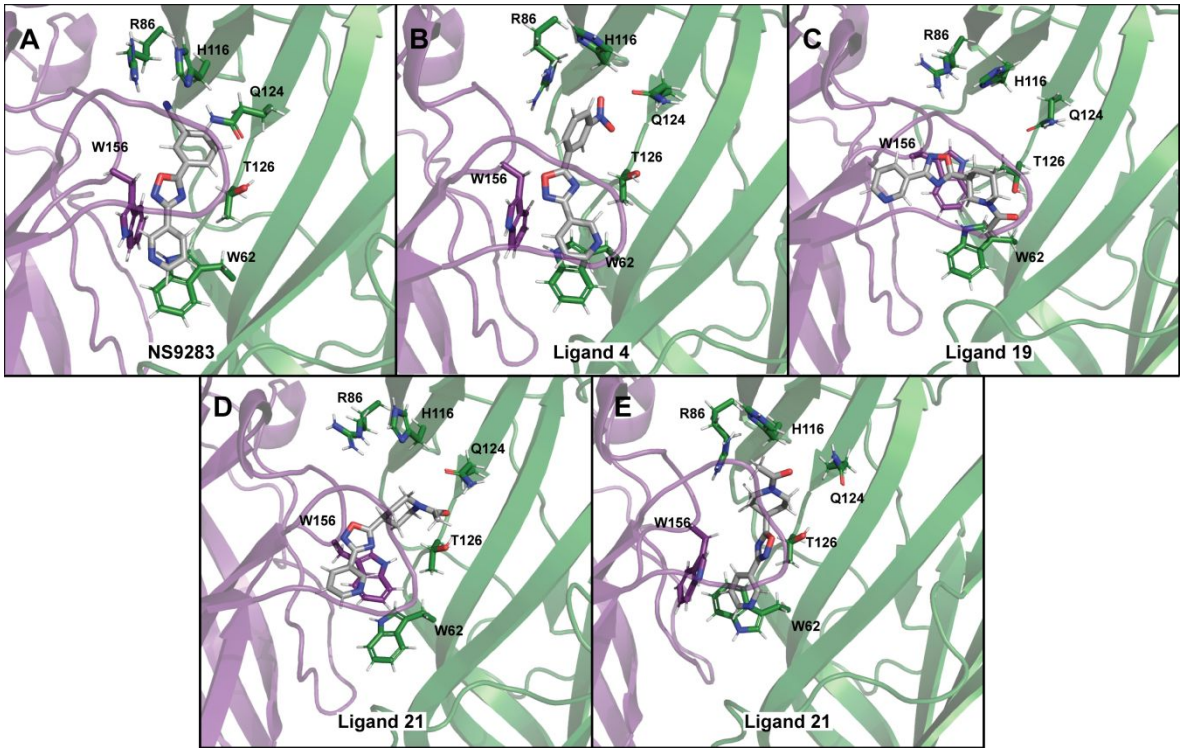

Figure 3. Selected conformations for NS9283 (**A**), ligand **4** (**B**), ligand **19** (**C**), and the two clusters of ligands **21** (**D, E**). The positive α subunit is represented in purple and the negative α subunit is represented in green.

Another striking feature of this binding conformation is the rotameric form of W156, which differs significantly from the native structure (Figure 4). In the case of ligand **4,** the conformation is similar to NS9283 (Figure 3B) and has a similar contact pattern (Supplementary Figure S3C and S3D), but it is less stable in the unbiased simulations (Supplementary Figure S1B). This is not surprising as this is the derivative with the closest functional activity to that of NS9283 (Table 1). On the other hand, the best pose for ligand **19**, which is inactive, is less stable in the unbiased simulations (Supplementary Figure S1C) and does not resemble the ones from NS9283 or ligand **4**, but instead appears oriented in the binding site in a horizontal fashion (Figure 3C), lacking both the key interactions present in the former ligands (Supplementary Figure S3E and S3F) and the conformational change of W156. Finally, since the two clusters obtained for ligand **21** (Figure 3D and 3E) had similar populations, none of them could be discarded *a priori*, thus both were analyzed for stability and contacts. The first conformation resulted to be less stable than the second (Supplementary Figure S1D and S1E). Furthermore, the contact pattern of the second pose (Supplementary Figure S3I and S3J) coincides better with the contacts of NS9283 and contains the alternative rotamer for W156, whereas in the first cluster the tryptophan is in its native like state.

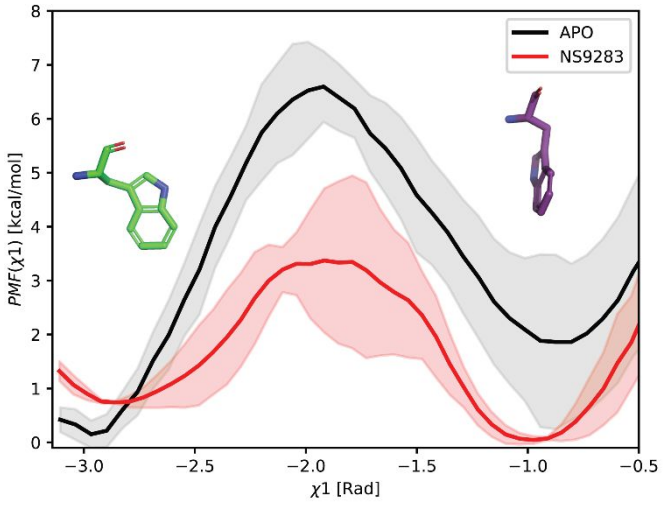

Figure 4. Potential of mean force on the tryptophan $_1$ angle with the native (green) and alternative (purple) conformations displayed over their corresponding basin. The PMF in the apo state (black) was calculated from US simulations, while the PMF in the bound state was calculated from REST simulation using the MBAR estimator (red). The shaded region corresponds to the standard deviation between the three replicas.

To ensure that the aforementioned alternative conformation is energetically accessible to the protein the potential of mean force (PMF) for this transition in the apo state was constructed using enhanced sampling. The resulting energy surface shows that, even though the native state is much more favorable, the alternative rotameric state is in a local minima basin, separated from the native conformation by a barrier of 7.06 kcal mol^{-1} ± 0.64 (Figure 4). For comparison, the PMF for the transition in the presence of NS9283 was obtained from the replica exchange with solute tempering (REST) simulations using the MBAR estimator. In the bound simulations the energy landscape is inverted, showing the alternative conformation as more favorable and a reduced barrier of XXX kcal mol-1. This suggest that the binding of NS9283 to the α4-α4 site allows for this conformational change to occur faster and without an energetic penalty.

Our previous studies on the $(\alpha4)_3(\beta2)_2$ nAChR have proved that mutations at either the principal face of the β2 subunit or the complementary face of the α4 subunit prevent NS9283 potentiation of ACh-elicited single channel currents, suggesting the drug targets the β2(+)-α4(-) subunit interface, the α4-α4 agonist site, or both sites.[22] Consistently, microscopic current studies have shown that LS α4β2 nAChR with mutant β2(+)-α4(-) interfaces are not potentiated by NS9283.[22] To assess the binding of the allosteric modulator in the β2(+)-α4(-) interface, REST simulations were performed using only NS9283 as a ligand. Clustering showed two main conformations for NS9283, neither of which shows strong interactions with the key conserved residues on the complementary face of the β2(+)-α4(-) interface or with the conserved tryptophan (W156) in loop B in the (+) side of the β2(+)-α4(-) interface (Supplementary Figure S4). This suggests that binding of NS9283 to the β2(+)-α4(-) subunit interface is not stable, compared to the one at the α4-α4 interface. These observations, together with

the findings that alanine substitution of a conserved tryptophan (W176) in the β2(+) side of β2(+)-α4(-) interfaces in LS α4β2 nAChR abolishes the allosteric effects of NS9283[22], support the possibility that the β2(+)/α4(-) interface may house components of the transduction machinery of the NS9283 binding site in the α4-α4 interface of the LS α4β2 nAChR.

CONCLUSIONS

The potentiation of neurotransmission at α4β2 nAChRs through ligands acting at other sites than the orthodox orthosteric α4/β2 site is a viable approach to fulfil the potential of this nicotinic receptor subtype as a drug target. In fact, such an approach is characterized by many favourable pharmacological properties, such as subtype and stoichiometry selectivity, alternative modulation mechanisms by decreasing receptor deactivation or desensitization, no or lower concomitant agonist dosage, minimal adverse effects. Nevertheless, a systematic development of classes of such ligands has not been extensively pursued to date. Proof of this is their small number with diverse pharmacological profiles and limited extent of *in vivo* studies. In this scenario, NS9283 stands out for its peculiar pharmacodynamic and pharmacokinetic properties highlighted by a number of studies *in vitro*, *ex vivo* and *in vivo*, these latter being recently exemplified by the reports on its combination with lower varenicline doses reducing alcohol consumption [24] or its administration alone or with the muscarinic agonist xanomeline rescuing nAChR signaling deficits in prefrontal cortex.[25,26] On the other side, knowledge of its selective molecular interactions with the unorthodox α4/α4 site, despite being deeply investigated, has not resulted in SAR studies aimed at building a wide class of analogues around this lead and confirming a common activity. Here, through an approach combining rational design and synthesis of NS9283 analogues, evaluation of their LS α4β2 selective ACh potentiation and computational studies of the interactions with the α4/α4 binding site, we have shown not only that the profile of LS α4β2 selective modulator acting at α4/α4 site, pertaining to NS9283, can be extended to other 5-(hetero)aryl substituted 3-(3-pyridyl)-1,2,4-oxadiazoles but also that the "chemical space" of the class can be enlarged to 1,2,4-oxadiazoles bearing heteroalicyclic

substituents, such as ligands **20** and **21**, which have a *N*-acylated 4-piperidinyl in position five respect to 3-cyanophenyl (NS9283), on condition of maintaining a correctly positioned HBA function on the cyclic substructure bound to C(5) of central oxadiazole. Consistently, computational studies on three ligands, namely the 3-cyanophenyl (NS9283), 3-nitrophenyl (**4**) and *N*-acetyl-4-piperidinyl (**21**) analogues, all endowed with ACh potentiation effect selectively exerted at LS α4β2 nAChR, suggest that all three bind to the α4/α4 site with poses resulting in similar contact patterns and, importantly, main interactions with the complementary (-) side, where H116 is critically involved, and with the W156 of the (+) side in a rotameric form significantly differing from the native one. These findings, besides providing a rationale for the present activity results, show that NS9283 is a good template to design new α4/α4 ligands and develop this class of compounds with focus on their promising therapeutic applications.

MATERIALS AND METHODS

Chemical synthesis. All chemicals and solvents were used as received from commercial sources or prepared as described in the literature. Flash chromatography purifications were performed using Biotage® Isolera® flash purification system using KP-Sil 32-63 μm 60 Å cartridges and Merck Silica Gel 60 (0.040-0.063 μm). TLC analyses were performed using 0.25mm silica gel plates on aluminium foil, containing a fluorescent indicator (Macherey-Nagel Alugram® SilG/UV 254) and visualized with UV light. Content of saturated aqueous solution of ammonia in eluent mixtures is given as v/v percentage. R_f values are given for guidance. 1H and 13C NMR spectra were recorded at 300 and 75 MHz using an FT-NMR spectrometer. Chemical shifts are reported in ppm relative to residual solvent ($CHCl_3$, MeOH or DMSO) as internal standard. Melting points were determined by Buchi Melting Point B-540 apparatus. The purity of lead compounds was measured by HPLC analysis using a Hewlett Packard HP1050 instrument. All compounds showed a purity ≥95% and retention times (R_t) are reported in Supplementary Information. 3-Cyanobenzoyl chloride was purchased from Sigma-Aldrich.

General procedure for the synthesis of compounds 27 and 53-56 (METHOD A). Hydroxylamine hydrochloride (2.0 eq) and $NaHCO_3$ (1.0 eq) or K_2CO_3 (2.0 eq) were dissolved in H_2O (20 mL) and the mixture was stirred until no effervescence occurred. Then, nitrile (1.3 eq) dissolved in EtOH (20 mL) was added. The resulting solution was stirred and heated at reflux for 3 h. Then, the solution was allowed to cool to rt, concentrated under reduce pressure to remove the ethanol and the aqueous residue was extracted with EtOAc (3 x 20 mL). The combined organics were dried with sodium sulphate and evaporated under reduced pressure to give the crude product which was purified as specified.

General procedure for the synthesis of compounds 28-44 and 49-52 (METHOD B). Carboxylic acid (1.0 eq) was dissolved in $SOCl_2$ (20 mL), and the mixture was stirred and heated at reflux for 2 h. Then, the solution was allowed to cool to rt and evaporated under reduced pressure to give the crude acyl chloride used for the next reaction without further purification.

General procedure for the synthesis of compounds 1-16 and 18-26 (METHOD C). Acyl chloride dissolved in toluene or pyridine was slowly added to a suspension of amidoxime in toluene or pyridine The resulting mixture was stirred and heated at reflux overnight. Then, the solution was allowed to cool to rt and concentrated under reduce pressure. The obtained crude was dissolved in ethyl acetate and washed with HCl 1M (2 x 10 mL), saturated $NaHCO_3$ solution (2 x 10 mL) and brine (2 x 10 mL). The organic phase was dried (Na_2SO_4) and evaporated under reduced pressure to give the crude product which was purified as specified.

Pyridine-3-amidoxime (27). Obtained from $NH_2OH{\cdot}HCl$ (3.47 g, 50.00 mmol), $NaHCO_3$ (2.10 g, 25.00 mmol) and 3-cyanopyridine (3.38 g, 32.50 mmol) using the general procedure **A**. Upon evaporation of the volatiles, the residue was purified by crystallization with DCM (10 mL). The desired product **27** was obtained as a white solid in 55% yield. mp 131.5-132.9 °C; R_f(DCM/MeOH 9:1) 0.40; ^{1}H NMR (300 MHz, DMSO-*d6*): δ 9.80 (bs, 1H, exchange with D_2O), 8.84 (dd, J = 2.3,

0.9 Hz, 1H), 8.54 (dd, *J* = 4.8, 1.7 Hz, 1H), 7.99 (ddd, *J* = 8.0, 2.3, 1.7 Hz, 1H), 7.38 (ddd, *J* = 8.0, 4.8, 0.9 Hz, 1H), 5.94 (bs, 2H, exchange with D_2O).

1-Formylpiperidine-3-carboxylic acid (45). Procedure adapted from literature.[29] A solution of formic acid (4.5 mL) and acetic anhydride (11 mL) was heated at 60 °C for 1 h and then cooled to 0 °C. Nipecotic acid (500 mg, 3.87 mmol) was added to the solution portion-wise. The mixture was allowed to warm to rt and stirred for 16 h. Then, the pH was adjusted to 7 using NaOH, concentrated under reduced pressure, diluted with DCM (5 mL) and filtered. The filtrate was concentrated under reduced pressure to give the crude product. Purification by crystallization in *i*PrOH (5 mL) gave the desired product **45** as a white solid in 76% yield. Mp 110.9-111.4 °C; R_f (DCM/MeOH 8:2) 0.46; ^{1}H NMR (300 MHz, $CDCl_3$) (50:50 mixture of rotamers): δ 11.13 (s, 1H), 8.09 (s, 1H), 4.58 (dd, *J* = 13.3, 4.2 Hz, 0.5H), 3.86 (ddd, *J* = 13.3, 5.8, 4.2 Hz, 0.5H), 3.78 – 3.64 (m, 1H), 3.53 (dd, *J* = 13.8, 8.2 Hz, 0.5H), 3.22 (ddd, *J* = 13.3, 9.1, 3.4 Hz, 0.5H), 3.10 (ddd, *J* = 13.8, 11.2, 3.4 Hz, 0.5H), 2.92 (dd, *J* = 13.3, 10.4 Hz, 0.5H), 2.61 – 2.39 (m, 1H), 2.06 – 1.92 (m, 1H), 1.92 – 1.77 (m, 1H), 1.76 – 1.60 (m, 1H), 1.60 – 1.40 (m, 1H).

1-Acetylpiperidine-3-carboxylic acid (46). Procedure adapted from literature.[30] Nipecotic acid (500 mg, 3.87 mmol) was added to the solution of DCM (9 mL) and acetic anhydride (0.37 mL, 3.87 mmol). The reaction mixture was stirred at rt overnight. Upon, the solution was concentrated under reduced pressure to give the crude compound. Purification by ion-exchange resin (Dowex 50WX4-400) in water gave 1-acetylpiperidine-3-carboxylic acid (**46**) as a clear oil in 80% yield. R_f (DCM/MeOH 8:2) 0.43; ^{1}H NMR (300 MHz, $CDCl_3$) (50:50 mixture of rotamers): δ 11.67 (bs, 1H), 4.06 (dd, *J* = 13.1, 3.9 Hz, 0.5H), 3.90 (dt, *J* = 13.1, 4.9 Hz, 0.5H), 3.72 (dd, *J* = 13.1, 3.9 Hz, 0.5H), 3.59 – 3.39 (m, 1H), 3.33 (dd, *J* = 13.1, 8.5 Hz, 0.5H), 3.23 (ddd, *J* = 13.0, 9.4, 3.3 Hz, 0.5H), 3.12 (ddd, *J* = 13.0, 9.4, 3.3 Hz, 0.5H), 2.52 – 2.34 (m, 1H), 2.12 (s, 1.5H), 2.06 (s, 1.5H), 2.02 – 1.90 (m, 1H), 1.89 – 1.70 (m, 1.5H), 1.70 – 1.58 (m, 0.5H), 1.56 – 1.38 (m, 1H).

1-Formylpiperidine-4-carboxylic acid (47). Procedure adapted from literature.[29] Formic acid (0.99 mL, 23.22 mmol) was added to acetic anhydride (2.2 mL, 23.22 mmol). The resulting solution was stirred and heated at 60 °C for 1 h. Then, the reaction mixture was gradually cooled to 5 °C, and isonipecotic acid (500 mg, 3.87 mmol) was added. The resulting mixture was stirred at rt for 16 h. Then, the mixture was concentrated under reduced pressure and 2-propanol (2 mL) was added. The suspension was filtered under cooled condition (6 °C) to obtained 1-formylpiperidine-4-carboxylic acid (**47**) as a white solid in 94% yield. M.p. 136-138 °C; R_f(DCM/Acetone 8:2) 0.38; ^{1}H NMR (300 MHz, $CDCl_3$): δ 8.04 (s, 1H), 4.32 – 4.14 (m, 1H), 3.73 – 3.56 (m, 1H), 3.25 – 3.11 (m, 1H), 3.00 – 2.87 (m, 1H), 2.78 – 2.58 (m, 1H), 2.08 – 1.94 (m, 2H), 1.80 – 1.60 (m, 2H).

1-Acetylpiperidine-4-carboxylic acid (48). Procedure adapted from literature.[30] Isonipecotic acid (500 mg, 3.87 mmol) was added to the solution of DCM (9 mL) and acetic anhydride (0.37 mL, 3.87 mmol). The reaction mixture was stirred at rt overnight. Then, the solution was concentrated under reduced pressure to give the crude compound. Purification by ion-exchange resin (Dowex 50WX4-400) in water gave 1-acetylpiperidine-4-carboxylic acid (**48**) as a pale yellow oil in 98% yield. R_f(DCM/MeOH 8:2) 0.45; ^{1}H NMR (300 MHz, $CDCl_3$): δ 9.88 (s, 1H), 4.48 – 4.37 (m, 1H), 3.88 – 3.77 (m, 1H), 3.16 (t, J = 12.5 Hz, 1H), 2.85 (t, J = 12.5 Hz, 1H), 2.76 – 2.56 (m, 1H), 2.10 (s, 3H), 2.05 – 1.94 (m, 2H), 1.82 – 1.58 (m, 2H).

***N*-Hydroxycyclohexanecarboximidamide (53).** Obtained from $NH_2OH{\cdot}HCl$ (3.47 g, 50.00 mmol), $NaHCO_3$ (2.10 g, 25.00 mmol) and cyclohexanecarbonitrile (3.55 g, 32.50 mmol) using the general procedure **A**. Upon evaporation of the volatiles, the residue was purified by flash chromatography to give **53** as a white solid in 46% yield. mp 90.4-92.7 °C; R_f(Cyclohexane/EtOAc 1:1) 0.17; ^{1}H NMR (300 MHz, DMSO-*d6*): δ 8.64 (s, 1H), 5.18 (s, 2H), 1.93 (tt, J = 11.9, 3.0 Hz, 1H), 1.81 – 1.53 (m, 5H), 1.40 – 1.02 (m, 5H).

***N*-Hydroxypiperidine-1-carboximidamide (54).** Obtained from $NH_2OH{\cdot}HCl$ (1.74 g, 25.00 mmol), $NaHCO_3$ (1.05 g, 12.50 mmol) and 1-piperidinecarbonitrile (1.79 g, 16.25 mmol) using the general procedure **A**. Upon evaporation of the volatiles, the residue was purified by flash chromatography to give **54** as a yellow oil in 53% yield. R_f(Cyclohexane/EtOAc 4:6) 0.33; ^{1}H NMR (300 MHz, $CDCl_3$): δ 4.82 (s, 1H), 4.70 - 4.20 (s, 2H), 3.32 (m, 4H), 3.03 (m, 6H).

***N*-Hydroxyfuran-3-carboximidamide (55).** Obtained from $NH_2OH{\cdot}HCl$ (3.47 g, 50.00 mmol), $NaHCO_3$ (2.10 g, 25.00 mmol) and 3-furonitrile (3.03 g, 32.50 mmol) using the general procedure **A**. Upon evaporation of the volatiles, the residue was purified by flash chromatography to give **55** as a yellow oil in 53% yield. R_f(Cyclohexane/EtOAc 1:1) 0.40; ^{1}H NMR (300 MHz, DMSO-*d6*): δ 9.58 (bs, 1H, exchange with D_2O), 7.65 (dd, J = 1.8, 0.8 Hz, 1H), 6.73 (dd, J = 3.4, 0.8 Hz, 1H), 6.50 (dd, J = 3.4, 1.8 Hz, 1H), 5.67 (bs, 2H, exchange with D_2O).

3-[(Hydroxyamino)(imino)methyl]benzoic acid (56). Obtained from $NH_2OH{\cdot}HCl$ (3.47 g, 50.00 mmol), K_2CO_3 (7.91 g, 50.00 mmol) and 3-cynobenzoic acid (4.78 g, 32.50 mmol) using the general procedure **A**. Upon evaporation of the volatiles, the residue was purified by flash chromatography to give **56** as a white solid in 94% yield. M.p. decomposes at 235°C; R_f (DCM/MeOH 9:1) 0.32; ^{1}H NMR (300 MHz, DMSO-*d6*): δ 9.47 (bs, 1H, exchange with D_2O), 8.20 (s, 1H), 7.91 (d, J = 7.7 Hz, 1H), 7.83 (d, J = 7.7 Hz, 1H), 7.44 (t, J = 7.7 Hz, 1H), 6.38 (s, 1H), 5.66 (bs, 1H, exchange with D_2O), 5.14 (bs, 1H, exchange with D_2O).

***N*-3-(Pyridine-3-yl)-1,2,4-oxadiazole (57).** Procedure adapted form literature.[31] To a solution of Pyridine-3-amidoxime (**27**) (500 mg, 3.65 mmol) in trimethyl orthoformate (10 mL) was added TFA (0.8 mL). The mixture was stirred for 5 min and then heated up to 60 °C and stirred for additional 30 min. Then, the mixture was allowed to cool to rt and concentrated under reduced pressure. The crude was diluted with $NaHCO_3$ (30 mL) and extracted with EtOAc (3 x 15 mL). The combined organics were washed with brine (10 mL), dried with sodium sulphate and evaporated under reduced pressure

to give pure **57** as a white solid in 63%. Mp 89.9-92.1 °C; R_f (Cyclohexane/EtOAc 6:4) 0.26; ^{1}H NMR (300 MHz, $CDCl_3$): δ 9.36 (s, 1H), 8.85 (s, 1H), 8.77 (d, *J* = 4.9, 1H), 8.39 (d, *J* = 8.0, 1H), 7.50 (dd, *J* = 8.0, 4.9 Hz, 1H).

Methyl 3-iodobenzoate (58). To a solution of 3-iodobenzoic acid (2.00 g, 8.06 mmol) in MeOH (50 mL) was assed dropwise concentrated H_2SO_4 (5 mL). The resulting solution was stirred and heated at reflux for 3 h. Then, the solution was allowed to cool to rt, diluted with Et_2O (100 mL) and washed with H_2O (2 × 10 mL), saturated $NaHCO_3$ (100 mL) and brine (100 mL). The organic layer was dried over sodium sulphate and evaporated under reduced pressure to give methyl 3-iodobenzoate (**58**) as a white solid in 93% yield. Mp 53.0-54.5 °C (lit., [164]54-56°C); R_f (Cyclohexane/EtOAc 7:3) 0.72; ^{1}H NMR (300 MHz, $CDCl_3$): δ 8.38 (s, 1H), 8.00 (d, *J* = 7.9 Hz, 1H), 7.88 (d, *J* = 7.9 Hz, 1H), 7.18 (t, *J* = 7.9 Hz, 1H), 3.92 (s, 3H).

3-(3-(pyridin-3-yl)-1,2,4-oxadiazol-5-yl)benzoic acid (17). Procedure adapted from literature.[31] A mixture of **57** (170 mg, 1.15 mmol), 3-iodobenzoate (**58**) (602 mg, 2.30 mmol), $Pd(OAc)_2$ (25 mg, 0.11 mmol), PPh_3 (60 mg, 0.22 mmol) and AgOAc (506 mg, 3.36 mmol) in toluene (27 mL) was stirred and heated at reflux overnight. Then, the suspension was allowed to cool to rt, and the solids were removed by filtration through Celite® and washed with EtOAc (3 x 25 mL). The combined organics were washed with brine (15 mL), dried over sodium sulphate and evaporated under reduced pressure to give the crude product. Purification by flash column chromatography on silica with 8:2 cyclohexane-ethyl acetate as eluent gave the desired compound as a white solid in 54% yield. Mp 123.2-125.2 °C; R_f (Cyclohexane/EtOAc 8:2) 0.23; ^{1}H NMR (300 MHz, $CDCl_3$): δ 9.42 (d, *J* = 1.2 Hz, 1H), 8.90 (s, 1H), 8.79 (dd, *J* = 4.8, 1.2 Hz, 1H), 8.55 – 8.38 (m, 2H), 8.31 (d, *J* = 7.9 Hz, 1H), 7.68 (t, *J* = 7.9 Hz, 1H), 7.47 (dd, *J* = 7.9, 5.2 Hz, 1H), 4.01 (s, 3H).

NaOH 1M (4 mL) was added to a solution of methyl 3-(3-(pyridin-3-yl)-1,2,4-oxadiazol-5-yl)benzoate (150 mg, 0.53 mmol) in MeOH (5 mL). The solution was stirred at rt for 2 h and then concentrated under reduced pressure. The residue was diluted with H_2O (20 mL) and extracted with

EtOAc (3 x 10 mL). The combined organics were dried over sodium sulphate and evaporated under reduced pressure to give **17** as a white solid in 78% yield. M.p. decomposes at 290°C ; R_f (DCM/MeOH 9:1) 0.21; ^{1}H NMR (300 MHz, DMSO-*d6*): δ 9.25 (s, 1H), 8.79 (d, *J* = 4.9 Hz, 1H), 8.68 (s, 1H), 8.45 (d, *J* = 7.9 Hz, 1H), 8.18 (d, *J* = 7.7 Hz, 1H), 8.12 (d, *J* = 7.7 Hz, 1H), 7.68 – 7.51 (m, 2H); ^{13}C NMR (75 MHz, DMSO-*d6*) δ 176.68, 168.12, 166.98, 152.79, 148.23, 142.39, 135.22, 134.36, 129.07, 129.04, 128.48, 124.81, 123.03, 122.61.

5-Phenyl-3-(pyridin-3-yl)-1,2,4-oxadiazole (1). Obtained from benzoyl chloride (**28**) (362 mg, 2.64 mmol), pyridine-3-amidoxime (**27**) (460 mg, 3.27 mmol) in pyridine (30 mL) using the general procedure **C**. Purification by flash column chromatography with 8:2 petroluem ether-ethyl acetate as eluent gave **1** as a white solid in 52%. Mp 138.6-141.0 °C; R_f (Cyclohexane/EtOAc 8:2) 0.21; ^{1}H NMR (300 MHz, $CDCl_3$): δ 9.41 (dd, *J* = 2.2, 0.9 Hz, 1H), 8.77 (dd, *J* = 4.9, 1.7 Hz, 1H), 8.45 (ddd, *J* = 8.0, 2.2, 1.7 Hz, 1H), 8.29 – 8.12 (m, 2H), 7.68 – 7.52 (m, 4H), 7.46 (ddd, *J* = 8.0, 4.9, 0.9 Hz, 1H); ^{13}C NMR (75 MHz, $CDCl_3$): δ 176.13, 167.00, 151.99, 148.70, 134.73, 133.00, 129.16, 128.20, 123.92, 123.62, 123.25.

3,5-di(Pyridin-3-yl)-1,2,4-oxadiazole (2). Obtained from pyridinoyl chloride (**29**) (997 mg, 7.04 mmol), pyridine-3-amidoxime (**27**) (779 mg, 5.68 mmol) in toluene (100 mL) using the general procedure **C**. Purification by flash column chromatography with 8:2 cyclohexane-ethyl acetate as eluent gave **28** as a white solid in 47% yield. Mp 126.3-127.4 °C; R_f(Cyclohexane/EtOAc 1:1) 0.31; ^{1}H NMR (300 MHz, DMSO-*d6*): δ 9.35 (d, *J* = 1.8 Hz, 1H), 9.26 (d, *J* = 1.8 Hz, 1H), 8.90 (dd, *J* = 4.8, 1.5 Hz, 1H), 8.81 (dd, *J* = 4.8, 1.5 Hz, 1H), 8.56 (dt, *J* = 8.0, 1.8 Hz, 1H), 8.45 (dt, *J* = 8.0, 1.8 Hz, 1H), 7.71 (dd, *J* = 8.0, 4.9 Hz, 1H), 7.65 (dd, *J* = 8.0, 4.9 Hz, 1H); ^{13}C NMR (75 MHz DMSO-*d6)*: δ 174.60, 167.05, 154.25, 152.99, 148.98, 148.27, 136.07, 135.19, 124.95, 124.83, 122.66, 120.28.

5-(2-nitrophenyl)-3-(pyridin-3-yl)-1,2,4-oxadiazole (3). Obtained from of 2-nitrobenzoyl chloride (**30**) (617 mg, 3.23 mmol), pyridine-3-amidoxime (**27**) (400 mg, 9.92 mmol) in pyridine (20 mL) using general procedure **C**. Purification by crystallization in EtOAc and Et_2O gave **3** as a white solid in 30% yield. Mp 105.2-106.2 °C; R_f (Cyclohexane/EtOAc 1:1) 0.26; ^{1}H NMR (300 MHz, $CDCl_3$): δ 9.37 (s, 1H), 8.78 (d, *J* = 4.7 Hz, 1H), 8.41 (dt, *J* = 8.1, 1.8 Hz, 1H), 8.12 – 7.96 (m, 2H), 7.88 – 7.76 (m, 2H), 7.47 (dd, *J* = 8.1, 4.7 Hz, 1H); ^{13}C NMR (75 MHz, $CDCl_3$): δ 173.00, 167.10, 152.22, 148.77, 148.66, 134.97, 133.28, 133.02, 131.41, 124.76, 123.78, 122.73, 118.83.

5-(3-nitrophenyl)-3-(pyridin-3-yl)-1,2,4-oxadiazole (4). Obtained from 3-nitrobenzoyl chloride (**31**) (983 mg, 5.30 mmol), pyridine-3-amidoxime (**27**) (586 mg, 4.27 mmol) in pyridine (30 mL) using the general procedure **C**. Purification by crystallization with EtOAc gave **4** as a light yellow solid in 59% yield. Mp 137.7-138.6 °C; R_f (Cyclohexane/EtOAc 1:1) 0.52; ^{1}H NMR (300 MHz, $CDCl_3$): δ 9.42 (d, *J* = 1.5 Hz, 1H), 9.09 (s, 1H), 8.80 (dd, *J* = 4.8, 1.5 Hz, 1H), 8.56 (d, *J* = 8.0 Hz, 1H) 8.52 – 8.40 (m, 2H), 7.81 (t, *J* = 8.0 Hz, 1H), 7.48 (dd, *J* = 8.0, 4.8 Hz, 1H); ^{13}C NMR (75 MHz, $CDCl_3$): δ 174.03, 167.43, 152.40, 148.76, 134.79, 133.59, 130.58, 127.32, 125.53, 123.73, 123.25, 122.70.

5-(4-nitrophenyl)-3-(pyridin-3-yl)-1,2,4-oxadiazole (5). Obtained from 4-nitrobenzoyl chloride (**32**) (1.20 g, 6.46 mmol), pyridine-3-amidoxime (**27**) (715 mg, 5.21 mmol) in toluene (100 mL) using the general procedure **C**. Purification by flash column chromatography with 7:3 cyclohexane-ethyl acetate as eluent gave **5** as light-yellow solid in 60% yield. Mp 178.2-178.5 °C; R_f (Cyclohexane/EtOAc 1:1) 0.40; ^{1}H NMR (300 MHz, $CDCl_3$): δ 9.41 (d, *J* = 1.6 Hz, 1H), 8.80 (dd, *J* = 4.8, 1.6 Hz, 1H), 8.51 – 8.37 (m, 5H), 7.48 (dd, *J* = 8.0, 4.8 Hz, 1H); ^{13}C NMR (75 MHz, $CDCl_3$): δ 174.12, 167.52, 152.41, 150.38, 148.75, 134.75, 129.30, 129.16, 124.42, 123.72, 122.67.

5-(3-fluorophenyl)-3-(pyridin-3-yl)-1,2,4-oxadiazole (6). Obtained from 3-fluorobenzoyl chloride (**33**) (455 mg, 2.87 mmol), pyridine-3-amidoxime (**27**) (394 mg, 2.87 mmol) in pyridine (20

mL) using general procedure **C**. Purification by flash column chromatography with 7:3 petroleum ether-ethyl acetate gave **6** as a light yellow solid in 26% yield. Mp 112.4-113.3 °C; R_f (Cyclohexane/EtOAc 7:3) 0.47; 1H NMR (300 MHz, CDCl3): δ 9.38 (d, *J* = 2.1 Hz, 1H), 8.76 (dd, *J* = 4.9, 1.7 Hz, 1H), 8.42 (dt, *J* = 8.0, 2.1 Hz, 1H), 8.01 (dt, *J* = 7.8, 1.2 Hz, 1H), 7.91 (ddd, *J* = 9.0, 2.7, 1.7 Hz, 1H), 7.55 (ddd, *J* = 8.4, 7.8, 5.5 Hz, 1H), 7.45 (dd, *J* = 8.0, 4.9 Hz, 1H), 7.32 (td, *J* = 8.4, 2.7 Hz, 1H); ^{13}C NMR (75 MHz, $CDCl_3$): δ 175.08, 167.14, 162.81 (d, *J* = 246.8 Hz), 152.12, 148.68, 131.07 (d, *J* = 8.3 Hz), 125.73 (d, *J* = 9.0 Hz), 124.02, 123.69, 123.04, 120.15 (d, *J* = 21.0 Hz), 115.23 (d, *J* = 24.09 Hz).

5-(3,4-difluorophenyl)-3-(pyridin-3-yl)-1,2,4-oxadiazole (7). Obtained from 3,4-difluorobenzoyl chloride (**34**) (1.00 g, 5.66 mmol), pyridine-3-amidoxime (**27**) (626 mg, 4.57 mmol) in pyridine (30 mL) using the general procedure **C**. Purification by flash column chromatography with 1:1 cyclohexane-ethyl acetate as eluent gave **7** as yellow solid in 93% yield. Mp 121.4-122.7 °C; R_f (Cyclohexane/EtOAc 4:6) 0.58; ^{1}H NMR (300 MHz, $CDCl_3$): δ 9.39 (s, 1H), 8.78 (dd, *J* = 4.8, 1.6 Hz, 1H), 8.42 (dt, *J* = 8.0, 1.6 Hz, 1H), 8.13 – 7.97 (m, 2H), 7.46 (dd, *J* = 8.0, 4.8 Hz, 1H), 7.43 – 7.30 (m, 1H); ^{13}C NMR (75 MHz, $CDCl_3$): δ 174.26, 167.17, 153.5 (dd, *J* = 257.6, 12.5 Hz), 152.17, 150.65 (dd, *J* = 251.5, 13.4 Hz), 148.66, 134.77, 125.19 (dd, *J* = 7.5, 4.0 Hz), 123.69, 122.92, 120.88 (dd, *J* = 6.8, 4.1 Hz), 118.55 (d, *J* = 18.4 Hz), 117.69 (dd, *J* = 19.6, 1.2 Hz).

5-(pyridin-2-yl)-3-(pyridin-3-yl)-1,2,4-oxadiazole (8). Obtained from picolinoyl chloride (**35**) (340 mg, 2.40 mmol), pyridine-3-amidoxime (**27**) (264 mg, 1.92 mmol) in pyridine (30 mL) using general procedure **C**. Purification by flash column chromatography with 7:3 to 6:4 DCM-ethyl acetate as eluent gave **8** as a white solid in 32% yield. Mp 131.7-133.3 °C; R_f (DCM/MeOH 95:5) 0.37; ^{1}H NMR (300 MHz, $CDCl_3$): δ 9.43 (dd, *J* = 2.2, 0.8 Hz, 1H), 8.87 (ddd, *J* = 4.8, 1.8, 0.8 Hz, 1H), 8.76 (dd, *J* = 4.9, 1.8 Hz, 1H), 8.53 – 8.43 (m, 1H), 8.30 (dd, *J* = 7.9, 1.1 Hz, 1H), 7.95 (td, *J* = 7.9, 1.8 Hz, 1H), 7.60 – 7.48 (m, 1H), 7.45 (ddd, *J* = 7.9, 4.9, 0.8 Hz, 1H); ^{13}C NMR (75 MHz, $CDCl_3$): δ 174.81, 167.32, 152.13, 150.82, 148.73, 143.35, 137.44, 134.95, 126.93, 124.35, 123.69, 122.96.

3-(pyridin-3-yl)-5-(pyridin-4-yl)-1,2,4-oxadiazole (9). Obtained from isonicotinoyl chloride (**36**) (460 mg, 3.25 mmol), pyridine-3-amidoxime (**27**) (357 mg, 2.60 mmol) in pyridine (25 mL) using general procedure **C**. Purification by crystallization with *i*PrOH gave **9** as a white solid in 41%. Mp 123.4-125.7 °C; R_f (DCM/MeOH 98:2) 0.44; ^{1}H NMR (300 MHz, CD_3OD): δ 9.32 (d, *J* = 2.2 Hz, 1H), 8.92 – 8.84 (m, 2H), 8.76 (dd, *J* = 4.9, 1.7 Hz, 1H), 8.58 (dt, *J* = 8.0, 2.0 Hz, 1H), 8.25 – 8.17 (m, 2H), 7.71 – 7.61 (m, 1H); ^{13}C NMR (75 MHz, CD_3OD): δ 174.34, 167.05, 151.42, 150.37, 147.33, 135.45, 131.41, 124.37, 123.24, 121.60.

5-(4-cyanophenyl)-3-(pyridin-3-yl)-1,2,4-oxadiazole (10). Obtained from 4-cyanobenzoyl chloride (**37**) (360 mg, 2.17 mmol), pyridine-3-amidoxime (**27**) (239 mg, 1.74 mmol) in pyridine (25 mL) using general procedure **C**. Purification by crystallization with *i*PrOH gave **10** as a white solid in 51% yield. Mp 179.9-180.8 °C; R_f (Cyclohexane/EtOAc 7:3) 0.21; ^{1}H NMR (300 MHz, $CDCl_3$): δ 9.41 (s, 1H), 8.85 – 8.73 (m, 1H), 8.45 (d, *J* = 6.5 Hz, 1H), 8.41 – 8.31 (m, 2H), 7.94 – 7.83 (m, 2H), 7.49 (t, *J* = 6.5 Hz, 1H); ^{13}C NMR (75 MHz, $CDCl_3$): 174.38, 167.44, 152.37, 148.72, 134.75, 132.96, 128.72, 127.59, 123.76, 122.74, 117.64, 116.50.

5-(4-fluorophenyl)-3-(pyridin-3-yl)-1,2,4-oxadiazole (11). Obtained from 4-fluorobenzoyl chloride (**38**) (340 mg, 2.14 mmol), pyridine-3-amidoxime (**27**) (294 mg, 2.14 mmol) in pyridine (20 mL) using general procedure **C**. Purification by flash column chromatography with 7:3 petroleum ether-ethyl acetate gave **11** as a white solid in 23% yield. Mp 144.6-156.4 °C; R_f (Cyclohexane/EtOAc 7:3) 0.47; ^{1}H NMR (300 MHz, CDCl3): δ 9.40 (s, 1H), 8.82 – 8.74 (m, 1H), 8.45 (dt, *J* = 8.2, 1.9 Hz, 1H), 8.30 – 8.21 (m, 2H), 7.48 (ddd, *J* = 8.2, 4.8, 0.9 Hz, 1H), 7.32 – 7.21 (m, 2H).; ^{13}C NMR (75 MHz, $CDCl_3$): δ 175.29, 166.98, 165.64 (d, *J* = 253.5 Hz), 151.80, 148.46, 134.99, 130.72 (d, *J* = 9.0 Hz), 123.79, 123.30, 120.30 (d, *J* = 3.0 Hz), 116.62 (d, *J* = 21.8 Hz).

3-(pyridin-3-yl)-5-(3,4,5-trifluorophenyl)-1,2,4-oxadiazole (12). Obtained from 3,4,5-trifluorobenzoyl chloride (**39**) (440 mg, 2.26 mmol), pyridine-3-amidoxime (**27**) (250 mg, 1.83

mmol) in toluene (45 mL) using general procedure **C**. Purification by flash column chromatography with 8:2 cyclohexane-ethyl acetate as eluent gave **12** as a white solid in 14% yield. Mp 152.0-153.2 °C; R_f(Cyclohexane/EtOAc 7:3) 0.49; ^{1}H NMR (300 MHz, $CDCl_3$): δ 9.38 (d, *J* = 1.4 Hz, 1H), 8.79 (dd, *J* = 4.9, 1.8 Hz, 1H), 8.42 (dt, *J* = 8.0, 1.8 Hz, 1H), 7.97 – 7.82 (m, 2H), 7.48 (ddd, *J* = 8.0, 4.9, 0.9 Hz, 1H); ^{13}C NMR (75 MHz, $CDCl_3$): δ 167.37, 153.44, 153.27, 152.37, 152.27, 150.37, 146.63, 148.70, 148.64, 134.85, 134.81, 123.76, 123.73, 122.70, 113.18, 113.07, 112.97, 112.86, 112.68.

3-(pyridin-3-yl)-5-(2,3,4,5-tetrafluorophenyl)-1,2,4-oxadiazole (13). Obtained from 2,3,4,5-tetrafluorobenzoyl chloride (**40**) (438 mg, 2.06 mmol), pyridine-3-amidoxime (**27**) (228 mg, 1.66 mmol) in toluene (40 mL) using general procedure **C**. Purification by flash column chromatography with 8:2 cyclohexane-ethyl acetate as eluent gave **13** as a white solid in 14% yield. Mp 112.1-113.0 °C; R_f(Cyclohexane/EtOAc 7:3) 0.37; ^{1}H NMR (300 MHz, $CDCl_3$): δ 9.40 (dd, *J* = 2.3, 0.9 Hz, 1H), 8.80 (dd, *J* = 4.9, 1.7 Hz, 1H), 8.44 (ddd, *J* = 8.0, 2.3, 1.7 Hz, 1H), 7.98 – 7.84 (m, 1H), 7.48 (ddd, *J* = 8.0, 4.9, 0.9 Hz, 1H); ^{13}C NMR (75 MHz, $CDCl_3$): δ 170.80, 167.00, 152.50, 152.31, 149.04, 149.01, 148.99, 148.96, 148.90, 148.87, 148.85, 148.82, 148.72, 148.61, 145.72, 145.69, 145.67, 145.64, 145.56, 145.53, 145.50, 145.40, 145.36, 145.31, 145.23, 145.20, 145.18, 145.15, 145.06, 145.04, 145.01, 143.59, 143.54, 143.43, 143.38, 143.33, 143.22, 143.17, 142.08, 142.04, 141.92, 141.88, 141.82, 141.69, 141.66, 140.20, 140.15, 140.03, 139.99, 139.94, 139.82, 139.77, 134.84, 134.72, 134.67, 123.78, 123.74, 123.66, 122.44, 112.05, 112.00, 111.95, 111.76, 111.72, 111.67, 108.85, 108.77, 108.66, 108.61.

5-(4-fluoro-3-nitrophenyl)-3-(pyridin-3-yl)-1,2,4-oxadiazole (14). Obtained from 4-fluoro-3-nitrobenzoyl chloride (**41**) (550 mg, 2.70 mmol), pyridine-3-amidoxime (**27**) (371 mg, 2.70 mmol) in toluene (25 mL) using general procedure **C**. Purification by flash column chromatography with 8:2 petroleum ether-ethyl acetate as eluent gave **14** as a light yellow solid in 13% yield. Mp 149.9-151.9 °C; R_f(Cyclohexane/EtOAc 7:3) 0.34; ^{1}H NMR (300 MHz, $CDCl_3$): δ 9.38 (d, *J* = 2.3 Hz, 1H), 8.93 (dd, *J* = 7.0, 2.3 Hz, 1H), 8.78 (dd, *J* = 4.9, 1.8 Hz, 1H), 8.49 (ddd, *J* = 8.7, 4.1, 2.2 Hz, 1H), 8.43 (dt,

J = 8.0, 1.9 Hz, 1H), 7.60 – 7.40 (m, 2H); ^{13}C NMR (75 MHz, $CDCl_3$): δ 173.16, 173.13, 167.42, 157.89 (d, *J* = 271.5 Hz), 152.39, 148.66, 134.86 (d, *J* = 9.8 Hz), 134.79, 126.41 (d, *J* = 2.3 Hz), 123.79, 122.60, 121.10 (d, *J* = 4.5 Hz), 119.98 (d, *J* = 21.75 Hz).

5-(3-fluoro-4-nitrophenyl)-3-(pyridin-3-yl)-1,2,4-oxadiazole (15). Obtained from 3-fluoro-4-nitrobenzoyl chloride (**42)** (440 mg, 2.16 mmol), pyridine-3-amidoxime (**27**) (297 mg, 2.16 mmol) in toluene (20 mL) using general procedure **C**. Purification by flash column chromatography with 7:3 to 8:2 gradient of petroleum ether-ethyl acetate as eluent gave **15** as a white solid in 16% yield. Mp 176.1-177.3 °C; R_f(Cyclohexane/EtOAc 7:3) 0.33; ^{1}H NMR (300 MHz, $CDCl_3$): 9.40 (d, *J* = 1.6 Hz, 1H), 8.81 (dd, *J* = 4.9, 1.6 Hz, 1H), 8.51 – 8.40 (m, 1H), 8.34 – 8.10 (m, 2H), 7.50 (dd, *J* = 8.0, 4.9 Hz, 1H); ^{13}C NMR (75 MHz, $CDCl_3$): δ 174.00, 173.08, 167.58, 155.55 (d, *J* = 265.5 Hz), 152.32, 148.55, 135.00, 130.03 (d, *J* = 9.0 Hz), 127.28 (d, *J* = 2.25 Hz), 124.22, 124.02 (d, *J* = 20.3 Hz), 122.57, 118.38 (d, *J* = 23.3 Hz).

5-(6-fluoropyridin-3-yl)-3-(pyridin-3-yl)-1,2,4-oxadiazole (16). Obtained from 6-fluoronicotinoyl chloride (**43**) (452 mg, 2.83 mmol), pyridine-3-amidoxime (**27**) (389 mg, 2.83 mmol) in pyridine (20 mL) using the general procedure **C**. Purification by flash column chromatography with 7:3 to 8:2 petroleum ether-ethyl acetate as eluent gave **16** as a white solid in 12% yield. M.p. 161.7-162.5 °C; R_f(Cyclohexane/EtOAc 7:3) 0.21; ^{1}H NMR (300 MHz, $CDCl_3$): δ 9.40 (dd, *J* = 2.2, 0.9 Hz, 1H), 9.12 (d, *J* = 2.5 Hz, 1H), 8.79 (dd, *J* = 4.9, 1.8 Hz, 1H), 8.61 (m, 1H), 8.44 (ddd, *J* = 8.0, 2.2, 1.8 Hz, 1H), 7.48 (ddd, *J* = 8.0, 4.9, 0.9 Hz, 1H), 7.17 (ddd, *J* = 8.6, 3.0, 0.9 Hz, 1H); ^{13}C NMR (75 MHz, $CDCl_3$): δ 173.20, 167.37, 165.65 (d, *J* = 235.5 Hz), 152.35, 148.73, 148.46, 144.68, 140.84 (d, *J* = 9.0 Hz), 134.84, 123.76, 122.37, 110.61 (d, *J* = 37.5Hz).

3-(3-(pyridin-3-yl)-1,2,4-oxadiazol-5-yl)piperidine-1-carbaldehyde (18). Obtained from 1-formylpiperidine-3-carbonyl chloride (**49**) (508 mg, 2.90 mmol), pyridine-3-amidoxime (**27**) (341 mg, 2.49 mmol) in pyridine (30 mL) using the general procedure **C**. Purification by flash column

chromatography with 8:2 ethyl acetate-petroleum ether + 1% TEA as eluent gave **18** as a yellow oil in 8% yield. R_f (EtOAc/petroleum ether 8:2) 0.33; ^{1}H NMR (300 MHz, $CDCl_3$) (50:50 mixture of rotamers): δ 9.27 (bs, 1H), 8.72 (bs, 1H), 8.32 (ddt, *J* = 8.0, 2.7, 1.8 Hz, 1H),), 8.10 (s, 0.5H), 8.07 (s, 0.5H), 7.42 (dd, *J* = 8.0, 4.8 Hz, 1H), 4.64 – 4.55 (m, 0.5H), 3.97 – 3.83 (m, 1H), 3.74 – 3.57 (m, 1H), 3.22 – 3.12 (m, 2.5H), 2.42 – 2.24 (m, 1H), 2.19 – 1.86 (m, 1.5H), 1.85 – 1.48 (m, 1.5H); ^{13}C NMR (75 MHz, $CDCl_3$) δ 179.77, 179.50, 166.34, 166.26, 161.13, 160.99, 151.90, 151.73, 148.36, 148.31, 134.97, 134.90, 123.79, 48.12, 45.77, 42.09, 39.88, 35.15, 34.23, 28.75, 28.41, 24.85, 23.01.

1-(3-(3-(pyridin-3-yl)-1,2,4-oxadiazol-5-yl)piperidin-1-yl)ethan-1-one (19). Obtained from 1-acetylpiperidine-3-carbonyl chloride (**50**) (585 mg, 3.08 mmol), pyridine-3-amidoxime (**27**) (341 mg, 2.49 mmol) in pyridine (30 mL) using the general procedure **C**. Purification by flash column chromatography with 8:2 to 9:1 ethyl acetate-petroleum ether as eluent gave **19** as a light yellow oil in 12% yield. R_f (EtOAc/petroleum ether 8:2) 0.38; ^{1}H NMR (300 MHz, $CDCl_3$) (50:50 mixture of rotamers): δ 9.25 (s, 1H), 8.71 (s, 1H), 8.37 – 8.25 (m, 1H), 7.41 (dd, *J* = 8.0, 4.8 Hz, 1H), 4.84 – 4.70 (m, 0.5H), 4.03 – 3.87 (m, 1H), 3.83 – 3.69 (m, 1H), 3.32 – 3.00 (m, 2.5H), 2.38 – 2.18 (m, 1H), 2.15 (s, 1.5H), 2.09 (s, 1.5H), 2.13 – 1.98 (m, 0.5H), 1.99– 1.84 (m, 1H), 1.79 – 1.51 (m, 1.5H); ^{13}C NMR (75 MHz, $CDCl_3$): δ 180.18, 179.91, 169.12, 166.29, 166.13, 151.81, 151.51, 148.27, 148.16, 135.07, 134.91, 123.81, 123.26, 48.64, 46.57, 43.97, 41.60, 35.11, 34.53, 28.50, 28.07, 24.75, 23.26, 21.48, 21.43.

4-(3-(pyridin-3-yl)-1,2,4-oxadiazol-5-yl)piperidin-1-carbaldehyde (20). Obtaine from 1-formylpiperidine-4-carbonyl chloride (**51**) (873 mg, 4.97 mmol), pyridine-3-amidoxime (**27**) (550 mg, 4.01 mmol) in pyridine (30 mL) using the general procedure **C**. Upon workup, the obtained solid was dissolved in DCM (20 mL) and washed with NaOH 20% (2 x 10 mL). Purification by flash column chromatography with 2:8 petroleum ether-ethyl acetate + 1% TEA as eluent gave **20** as a light yellow solid in 18% yield. M.p.103.9-105.5 °C; R_f (Petroleum ether/EtOAc + 1% TEA) 0.18; ^{1}H NMR (300 MHz, $CDCl_3$): δ 9.28 (s, 1H), 8.73 (dd, *J* = 4.9, 1.9 Hz, 1H), 8.32 (dt, *J* = 8.0, 1.9 Hz,

1H), 8.07 (s, 1H), 7.41 (dd, *J* = 8.0, 4.9 Hz, 1H), 4.32 (dtd, *J* = 13.5, 4.2, 1.3 Hz, 1H), 3.74 (dtd, *J* = 13.5, 4.2, 1.3 Hz, 1H), 3.41 – 3.21 (m, 2H), 3.11 – 2.94 (m, 1H), 2.31 – 2.12 (m, 2H), 2.04 – 1.80 (m, 2H); ^{13}C NMR (75 MHz, $CDCl_3$): δ 181.05, 166.40, 160.79, 152.03, 148.55, 134.75, 123.69, 123.00, 44.70, 38.64, 34.54, 29.70, 28.44.

1-(4-(3-(pyridin-3-yl)-1,2,4-oxadiazol-5-yl)piperidin-1-yl)ethan-1-one (21). Obtained from 1-acetylpiperidine-4-carbonyl chloride (**52**) (342.90 mg, 1.81 mmol), pyridine-3-amidoxime (**27**) (200 mg, 1.46 mmol) in pyridine (30 mL) using the general procedure **C**. Purification by flash column chromatography with 8:2 DCM-acetone as eluent gave **21** as a yellow solid in 20% yield. M.p. 105.3-106.3 °C; R_f(DCM/Acetone 8:2) 0.14; ^{1}H NMR (300 MHz, $CDCl_3$): δ 9.26 (dd, *J* = 2.0, 0.9 Hz, 1H), 8.71 (dd, *J* = 4.8, 1.9 Hz, 1H), 8.31 (dt, *J* = 8.0, 1.9 Hz, 1H), 7.40 (ddd, *J* = 8.0, 4.8, 0.9 Hz, 1H), 4.50 (dtd, *J* = 13.7, 4.2, 1.4 Hz, 1H), 3.89 (dtd, *J* = 13.7, 4.2, 1.4 Hz, 1H), 3.33 – 3.18 (m, 2H), 2.94 (ddd, *J* = 13.7, 11.1, 3.2 Hz, 1H), 2.24 – 2.13 (m, 2H), 2.11 (s, 3H), 2.02 – 1.78 (m, 2H); ^{13}C NMR (75 MHz, $CDCl_3$): δ 181.39, 168.92, 166.37, 152.05, 148.59, 134.65, 123.65, 123.00, 45.42, 40.52, 34.30, 29.53, 28.89, 21.41.

5-(cyclohex-1-en-1-yl)-3-(pyridin-3-yl)-1,2,4-oxadiazole (22). Obtained from cyclohex-1-ene-1-carbonyl chloride (**44**) (556 mg, 3.84 mmol), pyridine-3-amidoxime (**27**) (425 mg, 3.10 mmol) in pyridine (30 mL) using the general procedure **C**. Purification by flash column chromatography with 8:2 cyclohexane-ethyl acetate as eluent gave **22** as a light-yellow solid in 30% yield. M.p. 79.6-81.1 °C; R_f(Cyclohexane/EtOAc 8:2) 0.32; ^{1}H NMR (300 MHz, $CDCl_3$): δ 9.31 (dd, *J* = 2.1, 0.9 Hz, 1H), 8.72 (dd, *J* = 4.9, 1.9 Hz, 1H), 8.36 (dt, *J* = 8.0, 1.9 Hz, 1H), 7.41 (ddd, *J* = 8.0, 4.9, 0.9 Hz, 1H), 7.22 – 7.15 (m, 1H), 2.60 – 2.49 (m, 2H), 2.40 – 2.26 (m, 2H), 1.86 – 1.65 (m, 4H); ^{13}C NMR (75 MHz, $CDCl_3$): δ 176.97, 166.41, 151.71, 148.56, 139.04, 134.72, 123.96, 123.58, 123.54, 25.86, 24.54, 21.74, 21.29.

3-(3-cyclohexyl-1,2,4-oxadiazol-5-yl)benzonitrile (23). Obtained from 3-cyanobenzoyl chloride (1.00 g, 6.04 mmol), cyclohexanamidoxime (**53**) (693 mg, 4.87 mmol) in pyridine (30 mL) using the general procedure **C**. Purification by flash column chromatography with 8:2 cyclohexane-ethyl acetate as eluent gave **23** as a white solid in 43% yield. M.p. 62.0-62.6 °C; R_f (Cyclohexane/EtOAc 9:1) 0.36; ^{1}H NMR (300 MHz, $CDCl_3$): δ 8.42 (s, 1H), 8.34 (d, *J* = 7.9 Hz, 1H), 7.85 (d, *J* = 7.9 Hz, 1H), 7.66 (t, *J* = 7.9 Hz, 1H), 2.88 (tt, *J* = 11.4, 3.6 Hz, 1H), 2.14 – 2.01 (m, 2H), 1.93 – 1.55 (m, 5H), 1.51 – 1.24 (m, 3H); ^{13}C NMR (75 MHz, $CDCl_3$): δ 175.00, 172.97, 135.41, 131.77, 131.41, 130.07, 125.76, 117.43, 113.66, 35.84, 30.55, 25.69, 25.60.

3-(3-(piperidin-1-yl)-1,2,4-oxadiazol-5-yl)benzonitrile (24). Obtained from 3-cyanobenzoyl chloride (1.00 g, 6.04 mmol), piperidine-1-amidoxime (**54**) (697 mg, 4.87 mmol) in pyridine (30 mL) using the general procedure **C**. Purification by flash column chromatography with 8:2 cyclohexane-ethyl acetate as eluent gave **24** as a white solid in 54% yield. M.p. 87.8°C; R_f (Cyclohexane/EtOAc 8:2) 0.43; ^{1}H NMR (300 MHz, $CDCl_3$): δ 8.37 (s, 1H), 8.28 (d, *J* = 7.9 Hz, 1H), 7.83 (d, *J* = 7.9 Hz, 1H), 7.63 (t, *J* = 7.9 Hz, 1H), 3.49 (m, 4H), 1.71 – 1.63 (m, 6H); ^{13}C NMR (75 MHz, $CDCl_3$): δ 171.91, 170.75, 135.18, 131.63, 131.32, 129.91, 126.13, 117.60, 113.52, 47.00, 24.99, 24.10.

3-(3-(furan-3-yl)-1,2,4-oxadiazol-5-yl)-benzonitrile (25). Obtained from 3-cyanobenzoyl chloride (1.0 g, 6.04 mmol), furane-3-amidoxime (**55**) (614 mg, 4.87 mmol) in pyridine (30 mL) using the general procedure **C**. Purification by flash column chromatography with 8:2 cyclohexane-ethyl acetate as eluent gave **25** as a solid in 45% yield. M.p. 124.0-124.4 °C; R_f (Cyclohexane/EtOAc 1:1) 0.67; ^{1}H NMR (300 MHz, $CDCl_3$): δ 8.52 (s, 1H), 8.44 (dt, *J* = 7.9, 1.4 Hz, 1H), 7.90 (dt, *J* = 7.9, 1.4 Hz, 1H), 7.71 (t, *J* = 7.9 Hz, 1H), 7.68 - 7.65 (m, 1H), 7.24 (d, *J* = 3.5 Hz, 1H), 6.62 (dd, *J* = 3.5, 1.8 Hz, 1H); ^{13}C NMR (75 MHz, $CDCl_3$): δ 173.61, 162.08, 145.55, 141.85, 135.88, 131.99, 131.69, 130.21, 125.20, 117.35, 114.37, 113.92, 112.01.

3-(5-(3-cyanophenyl)-1,2,4-oxadiazol-3-yl)-benzoic acid (26). Obtained from 3-cyanobenzoyl chloride (1.50 g, 9.06 mmol), 3-amidoxime benzoic acid (**56**) (1.63 g, 9.06 mmol) in pyridine (15 mL) using the general procedure **C**. Purification by crystallization with MeOH (5 mL) gave **26** as a light yellow solid in 50% yield. M.p. 270-272 °C; R_f (DCM/MeOH 9:1) 0.38; ^{1}H NMR (300 MHz, DMSO-*d6*): δ 13.33 (s, 1H), 8.65 – 8.55 (m, 2H), 8.48 (d, *J* = 7.9 Hz, 1H), 8.30 (d, *J* = 7.9 Hz, 1H), 8.21 – 8.11 (m, 2H), 7.85 (t, *J* = 7.9 Hz, 1H), 7.72 (t, *J* = 7.9 Hz, 1H); ^{13}C NMR (75 MHz, DMSO-*d6*) δ 174.57, 168.27, 166.91, 137.13, 132.88, 132.80, 132.28, 131.96, 131.54, 131.31, 130.32, 128.26, 126.70, 124.91, 118.06, 113.29.

Functional assays in Xenopus oocytes

Adult female *Xenopus laevis* were purchased from *Xenopus* ONE (MI, USA). *Xenopus* care and experimental procedures were in accordance with the UK Home Office code of practice guidelines for the species.

The ligands reported (NS9283 and derivatives) were tested for potentiating effects on human α4β2, α5α4β2 or α7 nAChRs receptors expressed heterologously in *Xenopus* oocytes, which were isolated from adult female *Xenopus laevis* toads as previously described. [9] Human α4β2 receptors were expressed as either LS or HS α4β2 nAChR. To express LS αβ4 nAChRs, a mixture of 10 α4 : 1 β2 cDNAs was injected into the nucleus of oocytes, whereas for HS α4β2 receptors the cDNA ratio injected was 1 α4 : 10 β2. To express α4β2 or α7 nAChR, the nucleus of the oocytes was injected with 2-3 ng of either α4 and β2 or α7 cDNAs. To obtain expression of α5α4β2, 10 ng of fully concatenated cRNA α5α43β2 (subunit sequence α5β2α4β2α4) was injected into the cytoplasm of oocytes.

Two-electrode voltage-clamp recordings

Current responses were recoded using two-electrode voltage-clamp recording at a holding potential of -60 mV using an Oocyte Clamp OC-725C amplifier (Warner Instruments, USA) or the automated HiClamp system (Multi Channel Systems, Reutlingen, Germany), as previously described. [32]

Concentration-response curves for potentiation of ACh EC_{20} (30 μM for LS α4β2 and α7 nAChR and 3 μM for HS α4β2 and α5α4β2 nAChR) were obtained by normalizing the current responses (I) induced by the ligands in the presence ACh EC_{20} (30 μM) to the control responses induced by ACh EC_{20} using then equation $I_{AChEC20}$ + ligand/$_{IACh\ EC20}$. A minimum interval of 5 minutes was allowed between ligand applications to ensure reproducible recordings. The potentiation concentration-response relationships were analysed using non-linear regression in GraphPad (Prism 5, GraphPad, USA) by fitting the Hill equation (I([compound]) = Imax (1 / (1 + (EC_{50}/[compound])^n^{Hill})), where I is the response to a concentration of compound in the presence of ACh EC_{20}, Imax is the maximal response and corresponds the relative efficacy of the assayed ligand, EC_{50} is the concentration producing half-maximal potentiation, and n^{Hill} is the Hill coefficient.

Data points in plots or histograms represent the mean ± Standard error of the Mean (SEM) of 5-6 experiments carried out in at least three different batches of oocytes donors. The estimated EC_{50} or relative efficacy values are shown as mean ± SEM of 5-6 data sets. The data were analysed for statistical significance using one-way ANOVA, followed by a post hoc Dunnett's test and/or a post-hoc Bonferroni multiple comparison test to determine the level of significance between ligands and control (ACh) or ligands and NS9283.

Molecular dynamics simulations

System preparation

The α4β2 nAChR in the low sensitivity stoichiometry was obtained from the PDB database ID: 6CNK.[33] The structure was truncated and only the extracellular portion of the α4-α4 interface was retained. To compensate for the absence of the other subunits, harmonic restraints were applied to the five initial and final residues of each chain. Additionally, to validate the truncated construct, two additional simulations were carried using the full extracellular domain of the protein using the same harmonic restraints with NS9283 occupying the α4-α4 site and nicotine in the α4-β2 site. The coordinates for the ligands NS9283, ligand **4**, ligand **19**, and ligand **21** were prepared with the open-source software RDKit [34] and docked into the α4-α4 interface binding site using Autodock Vina [35] and the best ranked poses were used (Supplementary Figure S5). The topology for the ligands was produced with AmberTools22 [36] using the GAFF force field.[37] The best ranked docking pose was selected for simulations. The protein was parameterized with the Amber99SB force field,[38] solvated in a TIP3P water box,[39] and neutralized with 0.15 mM of NaCl. The system was then energy minimized and then equilibrated, first to 310K in an NVT ensemble and then to 1 atm in an NPT ensemble, both for 1 ns. All simulations were run in GROMACS 2021.5 patched with PLUMED version 2.8.0.[40,41]

Replica exchange with solute tempering (REST)

The replica exchange with solute tempering is a parallel tempering method, that is, a simulation method in which several replicas are run in parallel at different temperatures and every certain amount of steps an exchange is attempted between neighbouring replicas. This allows the system to explore the conformational space by overcoming barriers at higher temperatures and then exchanging back with the target temperature.[42,43] In this case the solute region, the part of the system whose temperature will be scaled, was defined as the ligand and 14 surrounding residues of the binding site (Y100, S155, W156, T157, Y197, C199, C200, and Y204 of the main (+) chain and W62, K64, R86,

H116, Q124, and T126 of the complementary (-) chain). To prevent the ligand dissociating from the binding site at high temperatures a flat bottom restraint at 8 Å from the center of mass of the binding site was applied to the ligand. The system simulated for 200 ns over a temperature range spanning from 310 K to 1000 K, distributed among 16 replicas, with attempted exchanges occurring every 1000 steps. This configuration was enough to provide good mixing between replicas (Supplementary Table S2). Subsequently, the trajectories at 310K were analyzed by clustering the ligand and selected binding site residues in order to extract representative conformations using the GROMOS algorithm.[44] Then, the selected conformations were used as a starting point for 200ns unbiased simulations in order to assess pose stability and contacts. To recover the free energy landscape of the tryptophan $\chi 1$ angle (the dihedral between N-CA-CB-CG), this collective variable was calculated for every replica and the samples were reweighted using the multistate Bennett acceptance ratio (MBAR) estimator implemented in pymbar[45]. All other analyses were performed using MDAnalysis.[46]

Umbrella sampling simulations

First, in order to generate a transition path for the umbrella sampling (US) a 10 ns steered molecular dynamics (SMD) simulation starting from the equilibrated native structure was run. During the simulation the heavy atoms of W156 were pulled towards the alternate conformation using a moving restraint on the root mean square deviation (RMSD) of the residue with respect to the NS9283 bound conformation. The restraint was shifted from 0.298445 to 0 nm with a force constant of 5000 kJ mol^{-1} nm^{-2} . From the resulting trajectory the frames with the closest tryptophan $_1$ angle to the 20 US restraint centres. US were run for 30 ns with a restraint on the corresponding centre and a force constant of 1000 kJ mol^{-1} nm^{-2} on the W156 $_1$ angle. The potential of mean force (PMFs) curve was constructed from the US trajectories using WHAM algorithm.[47]

ASSOCIATED CONTENT

Supporting Information

The Supporting Information is available free of charge on the ACS Publications website. The file type is PDF and contains ^{1}H and ^{13}C NMR spectra and HPLC chromatograms of **1-26** and computational data.

AUTHOR INFORMATION

Corresponding Authors

*E-mail: cristiano.bolchi@unimi.it

ORCID

Franco Viscarra. https://orcid.org/0000-0001-7891-7546

Isabel Bermudez. https://orcid.org/0000-0001-7692-1509.

Philip C. Biggin. https://orcid.org/0000-0001-5100-8836

Marco Pallavicini. https://orcid.org/0000-0003-3344-484X

Cristiano Bolchi. https://orcid.org/0000-0002-6726-9501

Alessandro Giraudo. https://orcid/0000-0002-5291-0837

Author Contributions

RA and FV equally contributed to this work and share first authorship.

CB and MP designed the project. RP carried out the chemical synthesis. IB and FV designed and carried out the functional assays. FV performed and analysed the MD simulations. PCB supervised the computational studies. CB, MP, IB, FV, PCB, RA and AG contributed to the rationalization of the results and preparation of the manuscript and figures. All authors have read and agreed to the published version.

Funding

This research was supported by Università degli Studi of Milan and Oxford Brookes University Research Excellence funding. Franco Viscarra was supported by Becas Chile for overseas PhD studentship.

Notes

The authors confirm that this article content has no conflict of interest.

Acknowledgments

We gratefully acknowledge support from OpenEye, Cadence Molecular Sciences for their free academic license for use of their applications and toolkits.

ABBREVIATIONS

ACh: acetylcholine

EC_{50}: ligand concentration producing half-maximal potentiation

Sample Availability

REFERENCES

[1] Terry, A. V.; Jones, K.; Bertrand, D. Nicotinic acetylcholine receptors in neurological and psychiatric diseases. *Pharmacol. Res.* **2023**, *191*, 106764.

[2] Matera, C.; Papotto, C.; Dallanoce, C.; De Amici, M. Advances in small molecule selective ligands for heteromeric nicotinic acetylcholine receptors. *Pharmacol. Res.* **2023**, *194,* 106813.

[3] F. Bavo, M. Pallavicini, R. Appiani, C. Bolchi, C. Determinants for α4β2 vs. α3β4 subtype selectivity of pyrrolidine-based nAChRs ligands: a computational perspective with focus on recent cryo-EM receptor structures. *Molecules*, **2021**, *26*, 3603.

[4] Bavo, F.; Pallavicini, M.; Gotti, C.; Appiani, R.; Moretti, M.; Colombo, S. F.; Pucci, S.; Viani, P.; Budriesi, R.; Renzi, M.; Fucile, S.; Bolchi, C. Modifications at C(5) of 2-(2-Pyrrolidinyl)-Substituted 1,4-Benzodioxane Elicit Potent α4β2 Nicotinic Acetylcholine Receptor Partial Agonism with High Selectivity over the α3β4 Subtype. *J. Med. Chem.* **2020**, *63*, 15668-15692.

[5] Bolchi, C.; Bavo, F.; Gotti, C.; Fumagalli, L.; Fasoli, F.; Binda, M.; Mucchietto, V.; Sciaccaluga, M.; Plutino, S.; Fucile, S.; Pallavicini, M. From pyrrolidinyl-benzodioxane to pyrrolidinyl-pyridodioxanes, or from unselective antagonism to selective partial agonism at α4β2 nicotinic acetylcholine receptor. *Eur. J. Med. Chem.* **2017**, *125*, 1132-1144.

[6] Braida, D.; Ponzoni, L.; Moretti, M.; Viani, P.; Pallavicini, M.; Bolchi, C.; Appiani, R.; Bavo, F.; Gotti, C.; Sala, M. Behavioural and pharmacological profiles of zebrafish administrated pyrrolidinyl benzodioxanes and prolinol aryl ethers with high affinity for heteromeric nicotinic acetylcholine receptors. *Psychopharmacol.* **2020**, *237*, 2317-2326.

[7] Appiani, R.; Pallavicini, M.; Hamouda, A. K.; Bolchi, C. Pyrrolidinyl benzofurans and benzodioxanes: Selective α4β2 nicotinic acetylcholine receptor ligands with different activity profiles at the two receptor stoichiometries. *Bioorg. Med. Chem. Lett.* **2022**, *65*, 128701.

[8] Nelson, M. E.; Kuryatov, A.; Choi, C. H.; Zhou, Y.; Lindstrom, J. Alternate stoichiometries of alpha4beta2 nicotinic acetylcholine receptors. *Mol. Pharmacol.* **2003**, *63*. 332-341.

[9] Moroni, M.; Zwart, R.; Sher, E.; Cassels, B. K.; Bermudez, I. Alpha4beta2 nicotinic receptors with high and low acetylcholine sensitivity: pharmacology, stoichiometry, and sensitivity to long-term exposure to nicotine. *Mol. Pharmacol.* **2006**, *70*, 755-768.

[10] Carbone, A. L.; Moroni, M.; Groot-Kormelink, P. J.; Bermudez, I. Pentameric concatenated $(\alpha4)_2(\beta2)_3$ and $(\alpha4)_3(\beta2)_2$ nicotinic acetylcholine receptors: subunit arrangement determines functional expression. *Br. J. Pharmacol.* **2009**, *156*, 970-981.

[11] Mazzaferro, S.; Benallegue, N.; Carbone, A.; Gasparri, F.; Vijayan, R.; Biggin, P. C.; Moroni, M.; Bermudez, I. Additional acetylcholine (ACh) binding site at α4/α4 interface of $(\alpha4\beta2)_2\alpha4$ nicotinic receptor influences agonist sensitivity. *J. Bio. Chem.* **2011**, *286*, 31043-31054.

[12] Wang, J.; Lindstrom, J. Orthosteric and allosteric potentiation of heteromeric neuronal nicotinic acetylcholine receptors. *Br. J. Pharmacol.* **2018**, *175*, 1805-1821.

[13] Malysz, J.; Dyhring, T.; Ahring, P. K.; Olsen, G. M.; Peters, D.; Gronlien, J. H.; Wteerstrand, C.; Ween, H.; Haakerud, M.; Thorin-Hagene, K.; Andersen, E.; Anderson, D. J.; Hu, M.; Kroeger, P. E.; Lee, C. H. L.; Gopalakrishnan, M.; Timmermann, D. B. In vitro pharmacological profile of a novel α4β2 positive allosteric modulator NS9283 (A-969933). *Biochem. Pharmacol.* **2009**, *78*, 919-920.

[14] Rode, F.; Munro, G.; Holst, D.; Nielsen, E. Ø.; Troelsen, K. B.; Timmermann, D. B.; Rønn, L. C. B.; Grunnet, M. Positive allosteric modulation of α4β2 nAChR agonist induced behaviour. *Brain Res.* **2012**, *1458*, 67-75.

[15] Timmermann, D. B.; Sandager-Nielsen, K.; Dyhring, T.; Smith, M.; Jacobsen, A. M.; Nielsen, E. Ø.; Grunnet, M.; Christensen, J. K.; Peters, D.; Kohlhaas, K.; Olsen, G. M.; Ahring, P. K. Augmentation of cognitive function by NS9283, a stoichiometry-dependent positive allosteric modulator of α2- and α4-containing nicotinic acetylcholine receptors. *Br. J. Pharmacol.* **2012**, *167*, 164-182.

[16] Grupe, M.; Jensen, A.A.; Ahring, P. K.; Christensen, J. K.; Grunnet, M. Unravelling the mechanism of action of NS9283, a positive allosteric modulator of $(\alpha4)_3(\beta2)_2$ nicotinic ACh receptors. *Br. J. Pharmacol.* **2013**, *168*, 2000-2010.

[17] Olsen, J. A.; Ahring, P. K.; Kastrup, J. S.; Gajhede, M.; Balle, T. Structural and Functional Studies of the Modulator NS9283 Reveal Agonist-like Mechanism of Action at α4β2 Nicotinic Acetylcholine Receptors. *J. Biol. Chem.* **2014**, *289*, 24911-24921.

[18] Wang, Z. J.; Deba, F.; Mohamed, T. S.; Chiara, D. C.; Ramos, K.; Hamouda, A. K. Unraveling amino acid residues critical for allosteric potentiation of $(\alpha4)_3(\beta2)_2$-type nicotinic acetylcholine receptor responses. *J. Biol. Chem.* **2017**, *292*, 9988-10001.

[19] Mohler, E. G.; Franklin, S. R.; Rueter, L. E. Discriminative-stimulus effects of NS9283, a nicotinic α4β2* positive allosteric modulator, in nicotine-discriminating rats. *Psychopharmacol.* **2014**, *231*, 67-74.

[20] Grupe, M.; Grunnet, M.; Bastlund, J. F.; Jensen, A. A. Targeting α4β2 Nicotinic Acetylcholine Receptors in Central Nervous System Disorders: Perspectives on Positive Allosteric Modulation as a Therapeutic Approach. *Basic Clin. Pharmacol. Toxicol.* **2015**, *116*, 187-200.

[21] Morales-Perez, C. L.; Noviello, C. M.; Hibbs, R. E. X-ray structure of the human α4β2 nicotinic receptor. *Nature* **2016**, *538*, 411-415.

[22] Mazzaferro, S.; Bermudez, I.; Sine, S. M. Potentiation of a neuronal nicotinic recptor via pseudo-agonist site. *Cell. Mol. Life Sci.* **2019**, *76*, 1151-1167.

[23] Liao, V. W. Y.; Kusay, A. S.; Balle, T.; Ahring, P. K. Heterologous expression of concatenated nicotinic ACh receptors: pros and cons of subunit concatenations and recommendations for construct designs. *Br. J. Pharmacol.* **2020**, *177*, 4275-4295.

[24] Wang, J.; Blasio, A.; Chapman, H. L.; Doebelin, C.; Liaw, V.; Kuryatov, A.; Giovanetti, S. M.; Lindstrom, J.; Lin, L.; Cameron, M. D.; Kamenecka, T. M.; Pomrenze, M. B.; Messing, R. O. Promoting activity of (α4)3(β2)2 nicotinic cholinergic receptors reduces ethanol consumption. *Neuropsychopharmacol.* **2020**, *45*, 301-308.

[25] Venkatesan, S.; Lambe, E. K. *Chrna5* is essential for a rapid and protected response to optogenetic release of endogenous acetylcholine in prefrontal cortex. *J. Neurosci.* **2020**, *40*, 7255-7268.

[26] Power, S. K.; Venkatesan, S.; Lambe, E. K. Xanomeline restores endogenous nicotinic acetylcholine receptor signaling in mouse prefrontal cortex. *Neuropsychopharmacol.* **2023**, *48*, 671-682.

[27] Jin, Z.; Khan, P.; Shin, Y.; Wang, J.; Lin, L.; Cameron, M. D.; Lindstrom, J. M.; Kenny, P. J.; Kamenecka, T. M. Synthesis and activity of substituted heteroaromatics as positive allosteric modulators for α4β2α5 nicotinic acetylcholine receptors. *Bioorg. Med. Chem. Lett.* **2014**, *24*, 674.

[28] Fowler, C. D.; Lu, Q.; Johnson, P. M.; Marks, M. J.; Kenny, P. J. Habenular α5 nicotinic receptor subunit signalling controls nicotine intake. *Nature* **2011**, *471*, 597-601.

[29] Shah, U. H.; Gaitonde, S. A.; Moreno, J. L.; Glennon, R. A.; Dukat, M.; González-Maeso, J. Revised pharmacophore model for 5-HT_{2A} receptor antagonists from the atypical antipsychotic agent risperidone. *ACS Chem. Neurosci.* **2019**, *10*, 2318-2331.

[30] R. J. Doll, A. K. Mallams, A. Afonso, D. F. Rane, F. G. Njoroge, R. R. Rossman (Schering Corporation NJ), *US 5891872A*, **1999**.

[31] Li, S.; Wan, P.; Ai, J.; Sheng, R.; Hu, Y.; Hu, Y. Palladium-catalyzed, silver-assisted direct C-5-H arylation of 3-substituted 1,2,4-oxadiazoles under microwave irradiation. *Adv. Synth. Catal.* **2017**, *359*, 772-778.

[32] Minguez, T.; Nielsen, N.; Shoemark, D. K.; Gotti, C.; Sessions, R. B.; Mulholland, A. J.; Bouzat, C.; Wonnacott, S.; Gallagher, T.; Bermudez, I.; Oliveira, A. S. A conserved arginine with non-conserved function is a key determinant of agonist selectivity in α7 nicotinic ACh receptors. *Br. J. Pharmacol.* **2021**, *178*, 1651-1668.

[33] Walsh Jr, R. M.; Roh, S. H.; Gharpure, A.; Morales-Perez, C. L.; Teng, J.; Hibbs, R. E. Structural principles of distinct assemblies of the human α4β2 nicotinic receptor. *Nature* **2018**, *557*, 261-265.

[34] Landrum, G. RDKit: Open-source cheminformatics. https://www.rdkit.org,. https://doi.org/10.5281/zenodo.591637

[35] Trott, O.; Olson, A. J. AutoDock Vina: improving the speed and accuracy of docking with a new scoring function, efficient optimization, and multithreading. *J. Comput. Chem.* **2010**, *31*, 445-461.

[36] Case,D.A.; Aktulga,H.M.; Belfon,K.;et al. Amber2022; University of California, San Francisco, 2022.

[37] Wang, J.; Wolf, R. M.; Caldwell, J. W.; Kollman, P. A.; Case, D. A. Development and testing of a general amber force field. *J. Comput. Chem.* **2004**, *25*, 1157-1174.

[38] Hornak, V.; Abel, R.; Okur, A.; Strockbine, B.; Roitberg, A.; Simmerling, C. Comparison of multiple Amber force fields and development of improved protein backbone parameters. *Proteins*, **2006**, *65*, 712-725.

[39] Jorgensen, W. L.; Chandrasekhar, J.; Madura, J. D.; Impey, R. W.; Klein, M. L. Comparison of simple potential functions for simulating liquid water. *J. Chem. Phys.* **1983**, *79*, 926-935.

[40] Vanommeslaeghe, K.; MacKerell Jr, A. D. CHARMM additive and polarizable force fields for biophysics and computer-aided drug design. *Biochim. Biophys. Acta* **2015**, *1850*, 861-871.

[41] Tribello, G.A.; Bonomi, M.; Branduardi, D.; Camilloni, C.; Bussi, G. PLUMED 2: new feathers for an old bird. *Comput. Phys. Comm.* **2014**, *185*, 604-613.

[42] Liu, P.; Byungchan, K.; Friesner, R. A.; Berne, B. J. Replica exchange with solute tempering: a method for sampling biological systems in explicit water. *PNAS* **2005**, *102*, 13749-13754.

[43] Wang, L.; Friesner, R. A.; Berne, B. J. Replica exchange with solute scaling: a more efficient version of replica exchange with solute (REST2). *J. Phys. Chem. B* **2011**, *115*, 9431-9438.

[44] Daura, X.; Gademann, K.; Jaun, B.; Seebach, D.; van Gusteren, W. F.; Mark, A. E. Peptide folding: when simulation meets experiment. *Angew. Chem. Int. Ed.* **1999**, *38*, 236-240.

[45] Shirts, M.R.; Chodera, J.D. Statistically optimal analysis of samples from multiple equilibrium states. J. Chem. Phys. **2008**, 129:124105.

[46] Michaud-Agrawal, N.; Denning, E. J.; Woolf, T. B.; Beckstein, O. MDAnalysis: a toolkit for the analysis of molecular dynamics simulations. *J. Comput. Chem.* **2011**, *32*, 2319-2327.

[47] Bauer, D. WHAM – An efficient weighted histogram analysis implementation written in Rust. Zenodo. https://doi.org/10.5281/zenodo.1488597

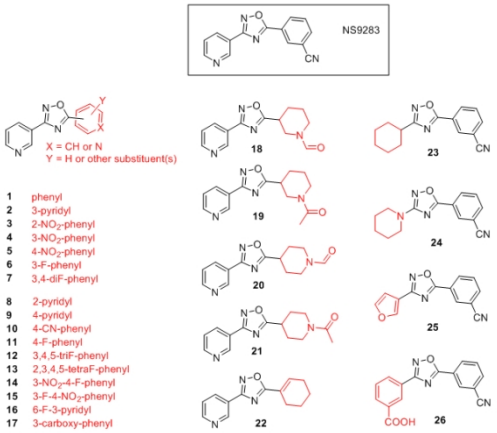

338x190mm (96 x 96 DPI)

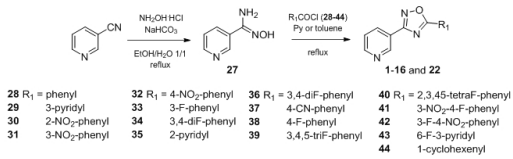

28	R_1 = phenyl	**32**	R_1 = 4-NO_2-phenyl	**36**	R_1 = 3,4-diF-phenyl	**40**	R_1 = 2,3,45-tetraF-phenyl
29	3-pyridyl	**33**	3-F-phenyl	**37**	4-CN-phenyl	**41**	3-NO_2-4-F-phenyl
30	2-NO_2-phenyl	**34**	3,4-diF-phenyl	**38**	4-F-phenyl	**42**	3-F-4-NO_2-phenyl
31	3-NO_2-phenyl	**35**	2-pyridyl	**39**	3,4,5-triF-phenyl	**43**	6-F-3-pyridyl
						44	1-cyclohexenyl

338x190mm (96 x 96 DPI)

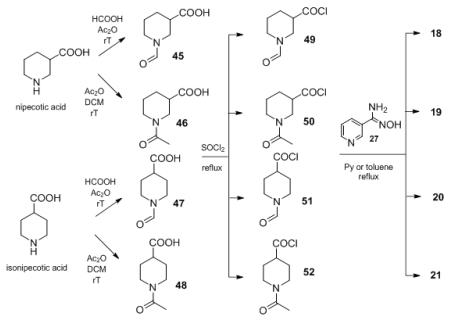

338x190mm (96 x 96 DPI)

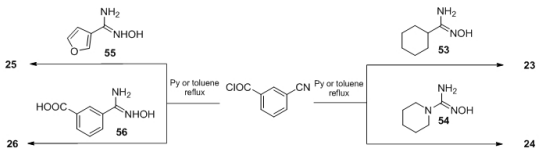

338x190mm (96 x 96 DPI)

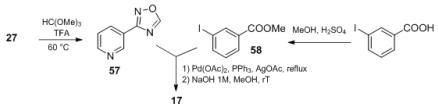

338x190mm (96 x 96 DPI)

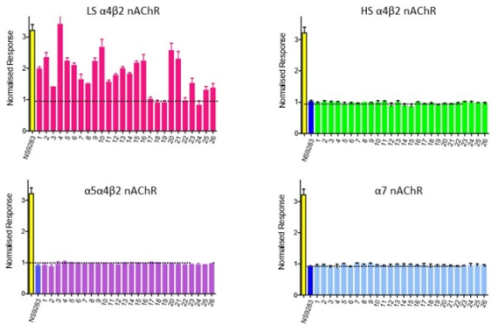

338x190mm (96 x 96 DPI)

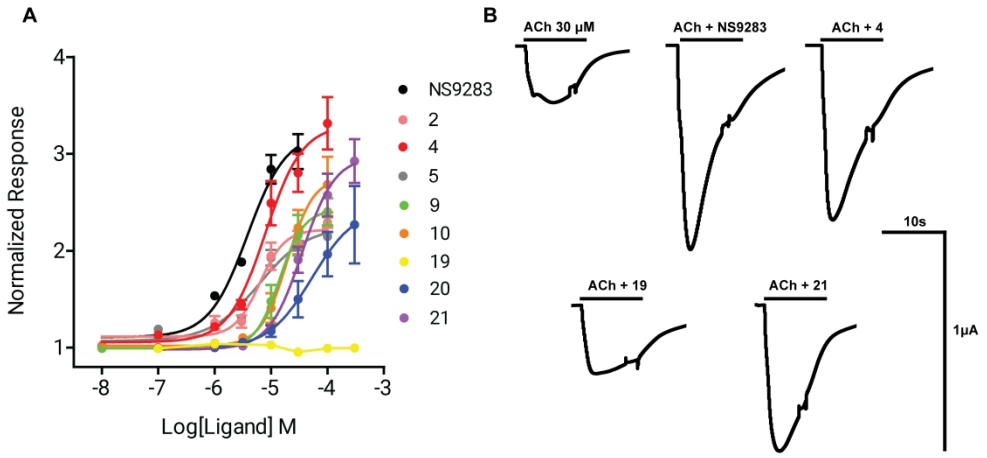

205x100mm (600 x 600 DPI)

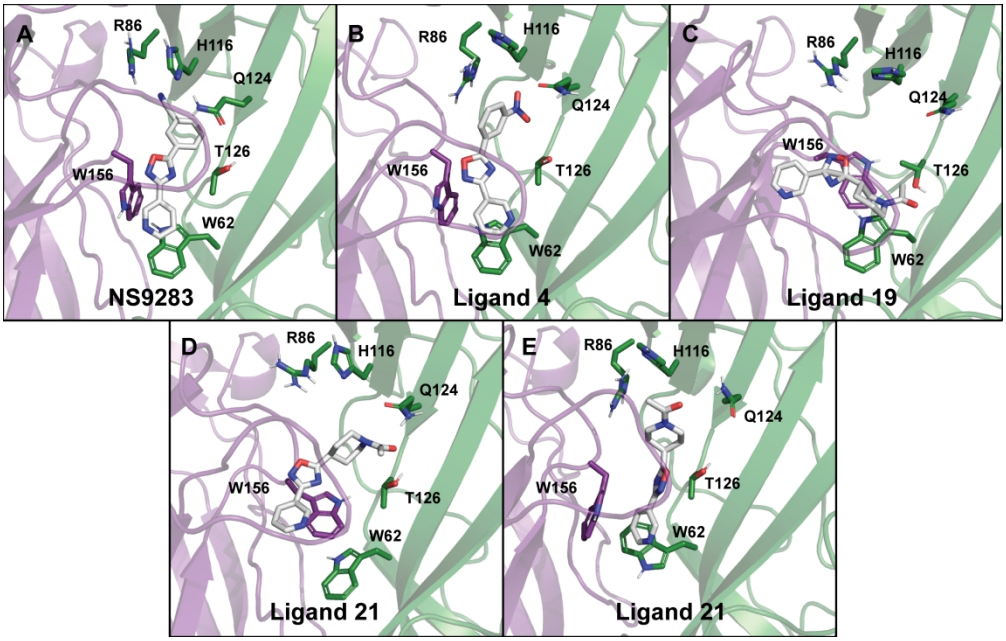

177x112mm (600 x 600 DPI)

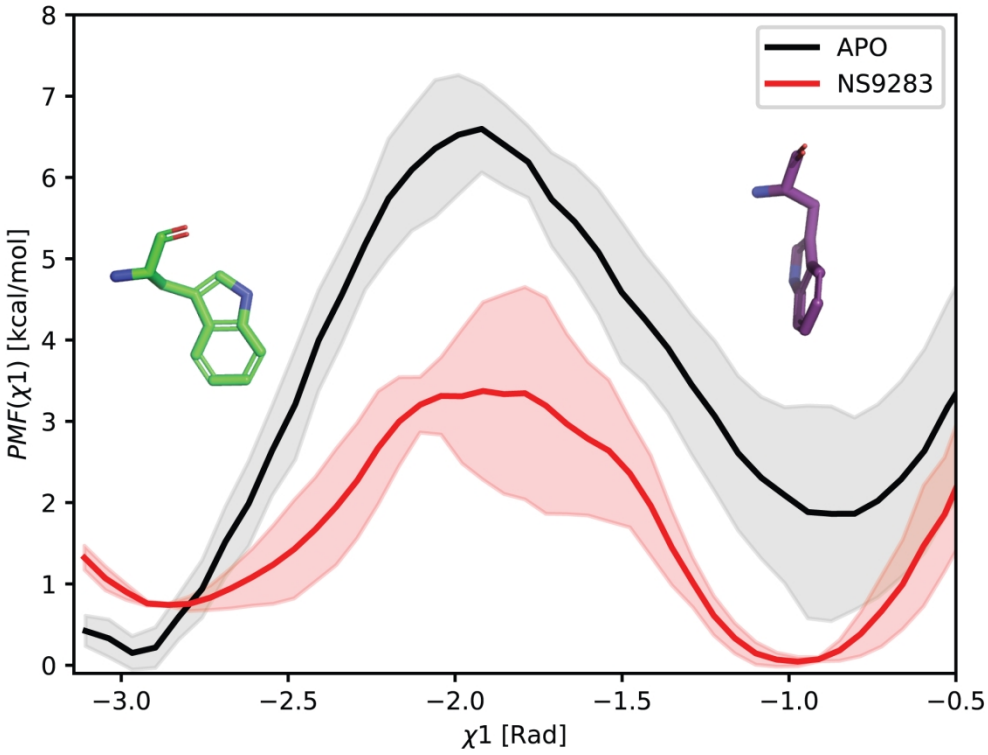

88x71mm (600 x 600 DPI)

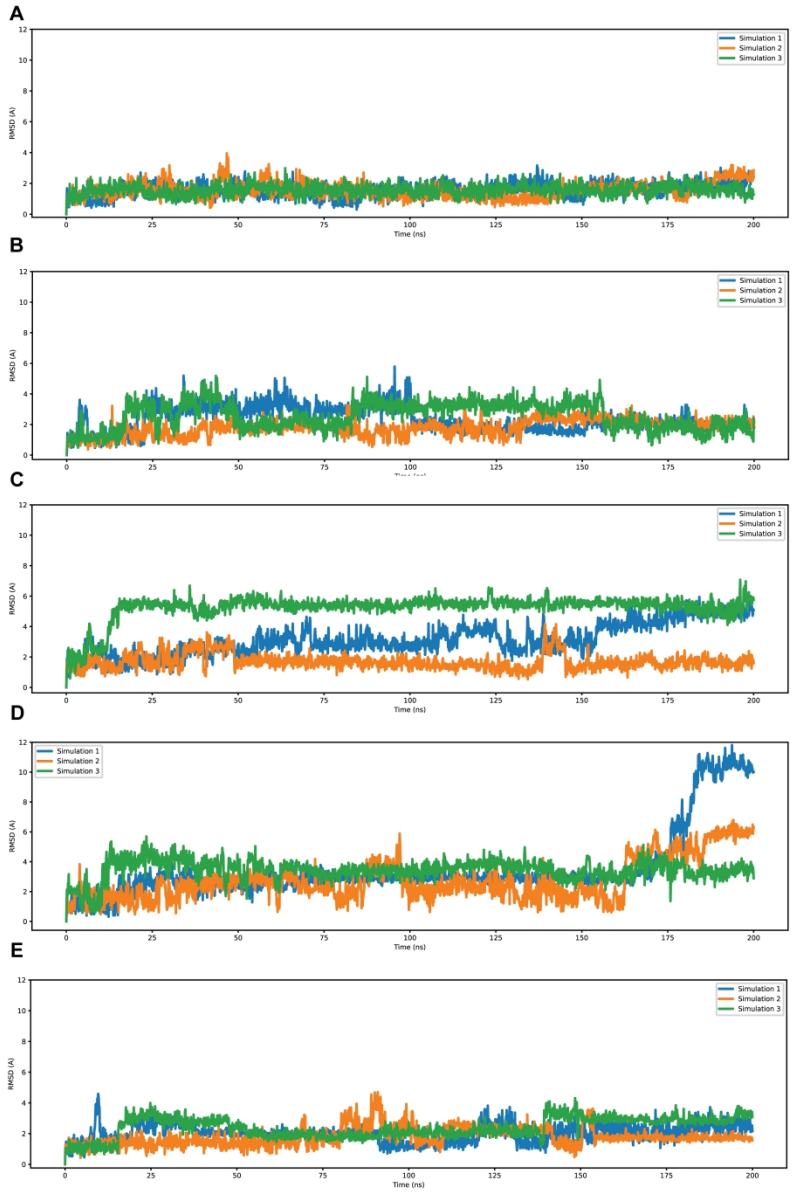

177x252mm (600 x 600 DPI)

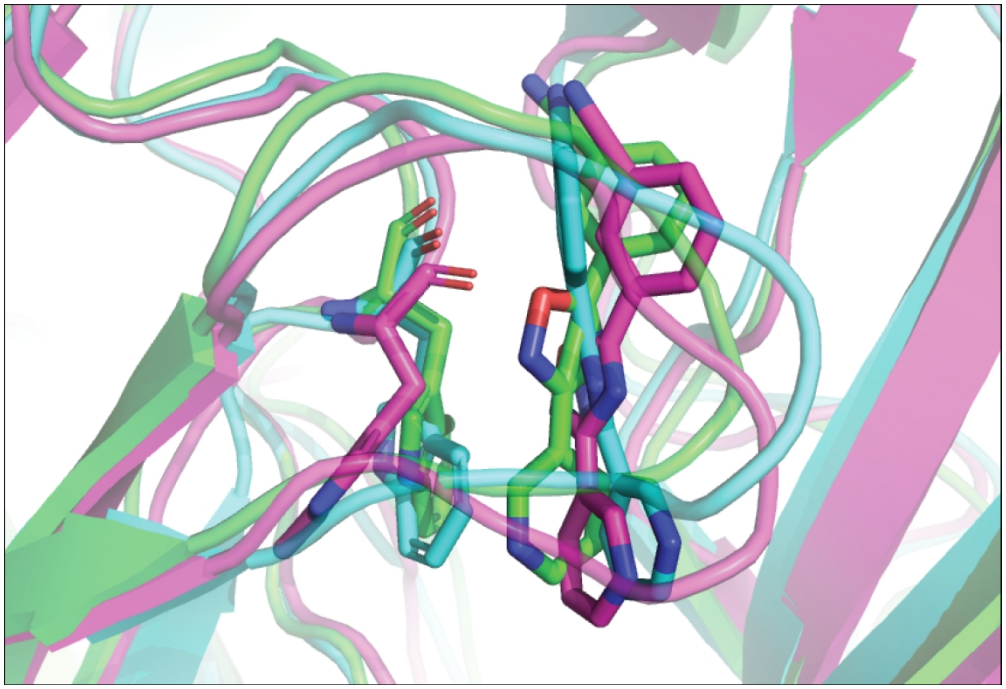

177x120mm (600 x 600 DPI)

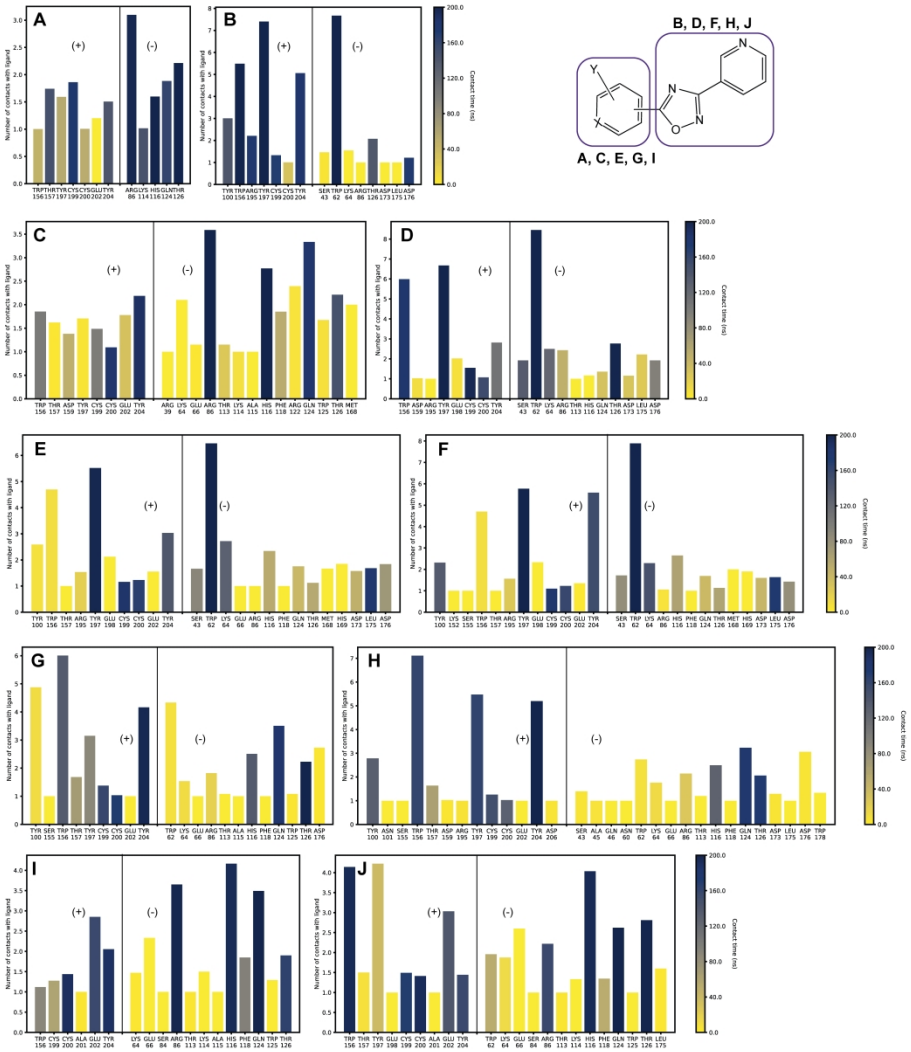

177x232mm (600 x 600 DPI)

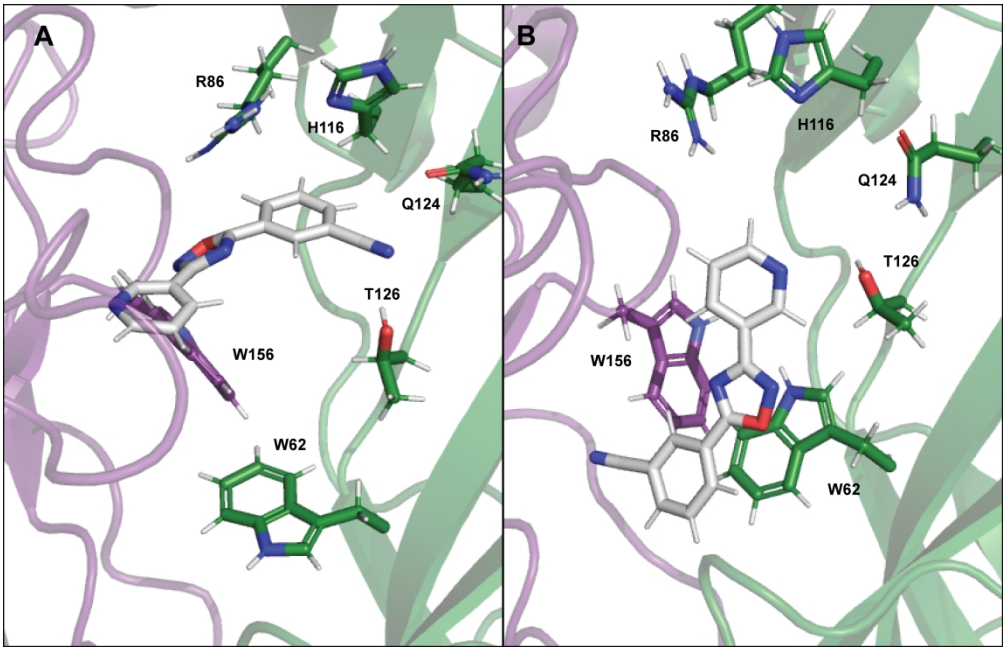

177x114mm (600 x 600 DPI)

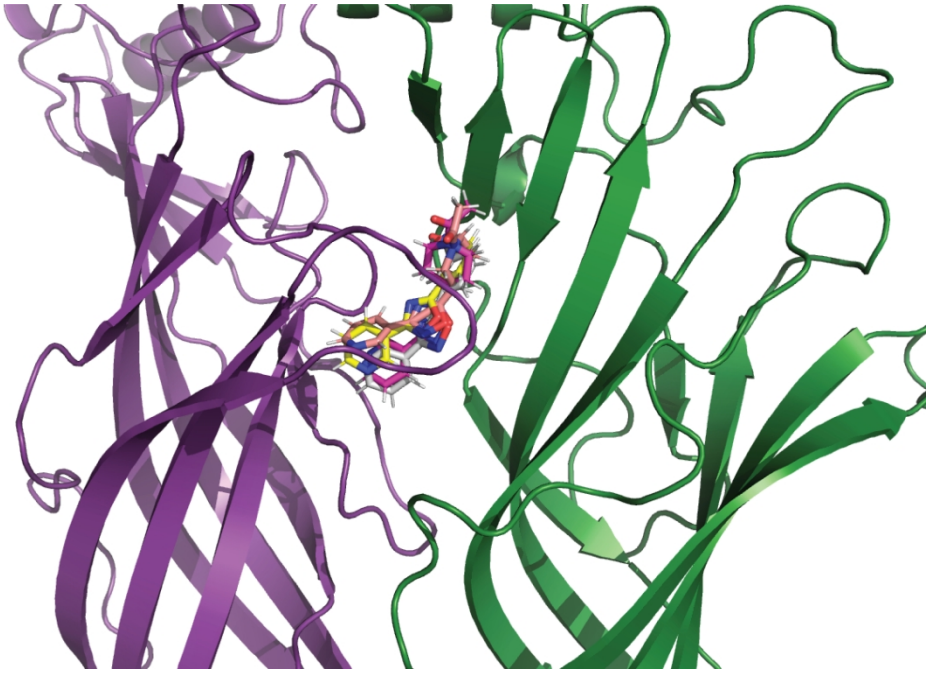

177x118mm (600 x 600 DPI)

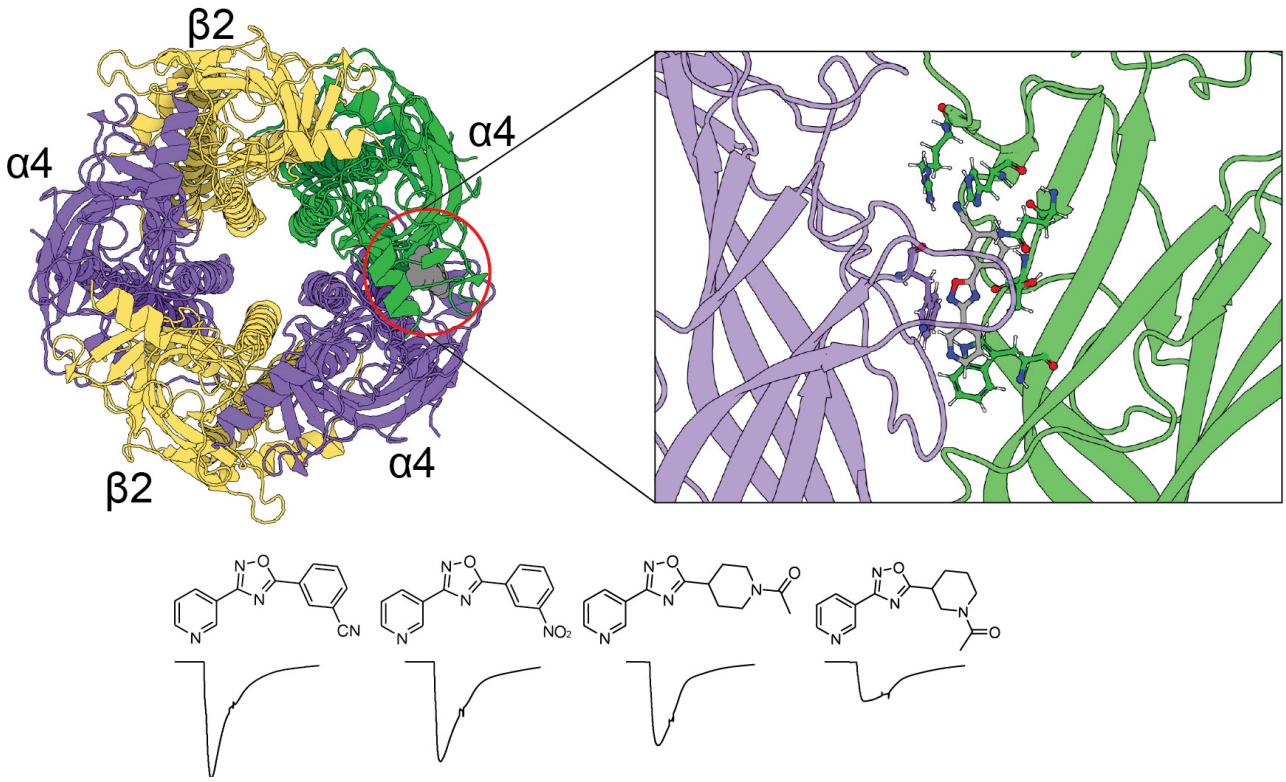
β2
α4
α4
α4
β2
CN
NO2
N
O